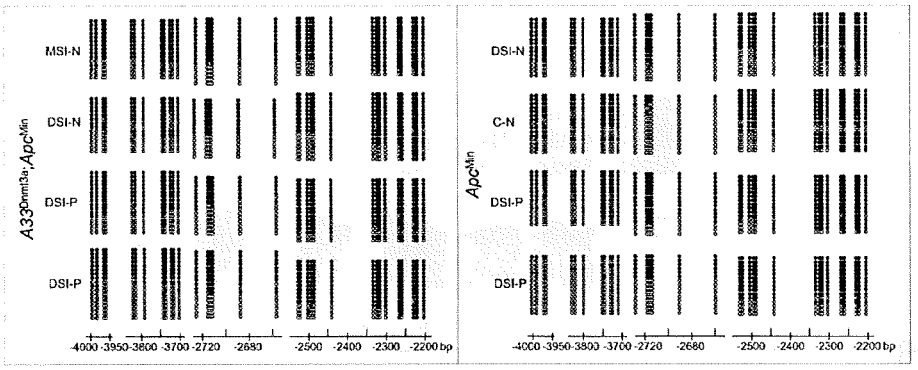

Supplementary Figure 4. *Igf2/H19* methylation is not affected in IECs of *A33*^{Dnmt3a};*Apc*^{Min} mice. Bisulfite sequencing analysis of *Igf2/H19* in polyps (P) and adjacent normal mucosa (N) from the distal small intestine (DSI) and colon (C) of *A33*^{Dnmt3a};*Apc*^{Min} and *Apc*^{Min} mice. Horizontal lines represent results from 1 individual sequence with unmethylated (open circle) and methylated (closed circle) CpG residues indicated, and located at the indicated nucleotide position relative to the transcriptional start site. Each block of sequence represents data from a single biological sample.

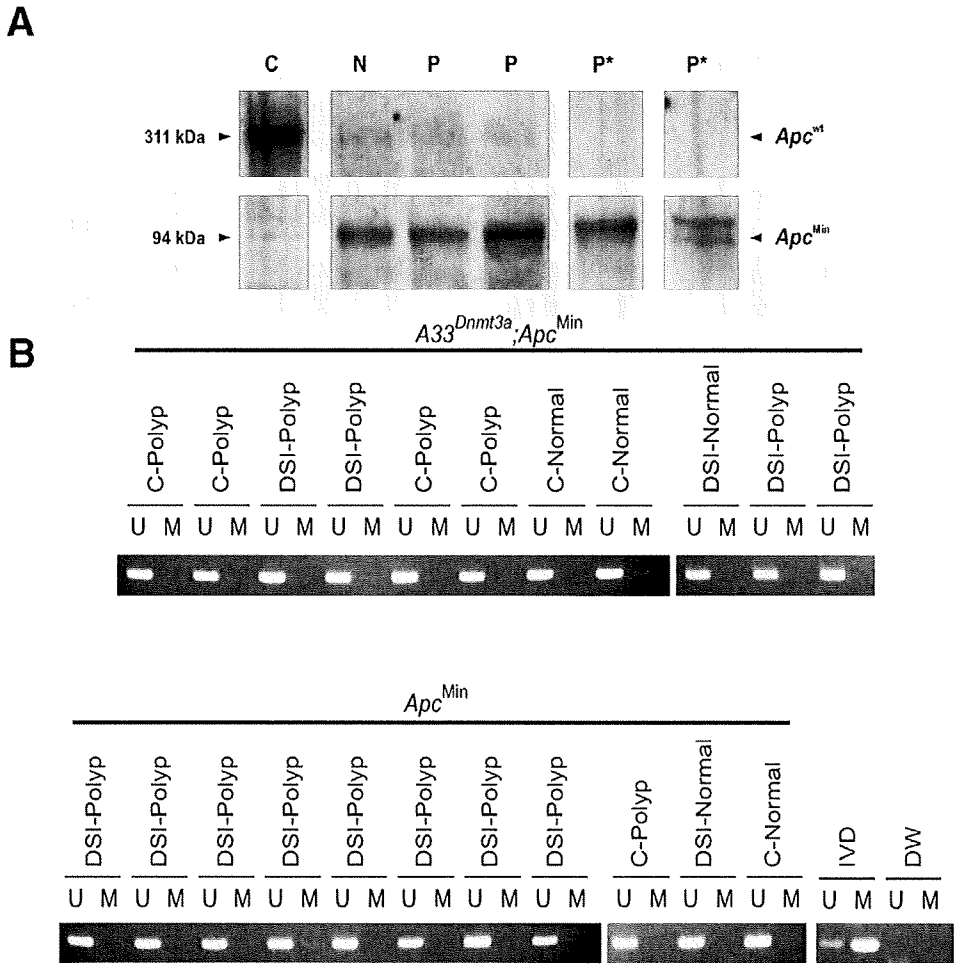

Supplementary Figure 5. Maintenance of *Apc* heterozygosity in the absence of *Apc* promoter methylation in tumors of $A33^{Dnmt3a}$;Apc^{Min} mice. (*A*) Western blot analysis of tissue lysates from normal (N) mucosa and individual polyps (P) from $A33^{Dnmt3a}$;Apc^{Min} mice. IECs prepared from normal mucosa or polyp samples were homogenized in buffer (30 mmol/l Tris-Cl [pH 7.4]; 250 mmol/l NaCl, 0.1% Triton X-100, 50 mmol/l EDTA, 50 mmol/l NaF, 1× complete protease inhibitor; Roche) using a mechanical homogenizer. Samples were cleared by centrifugation in a bench-top centrifuge. The protein concentration of the cleared sample was estimated using a Bradford assay kit (Bio-Rad). Total protein (40 μg) was loaded onto a 3%–8% gradient Tris-acetate gel and electrophoresed at 150 V for 2 hours. Proteins were transferred onto nitrocellulose membrane and probed with an Apc antiserum raised against the C-terminal part of the full-length protein and visualized using ECL reagents (GE Biosciences). Each lane represents 1 individual polyp and P* denotes lesions consistent with LOH for *Apc*. (*B*) Methylation sensitive PCR analysis of *Apc* in DNA extracted from polyps and normal mucosa in the distal small intestine (DSI) and colon (C) from Apc^{Min} and $A33^{Dnmt3a}$;Apc^{Min} mice. DW, no template control; IVD, in vitro methylated DNA; M, methylated; U, unmethylated.

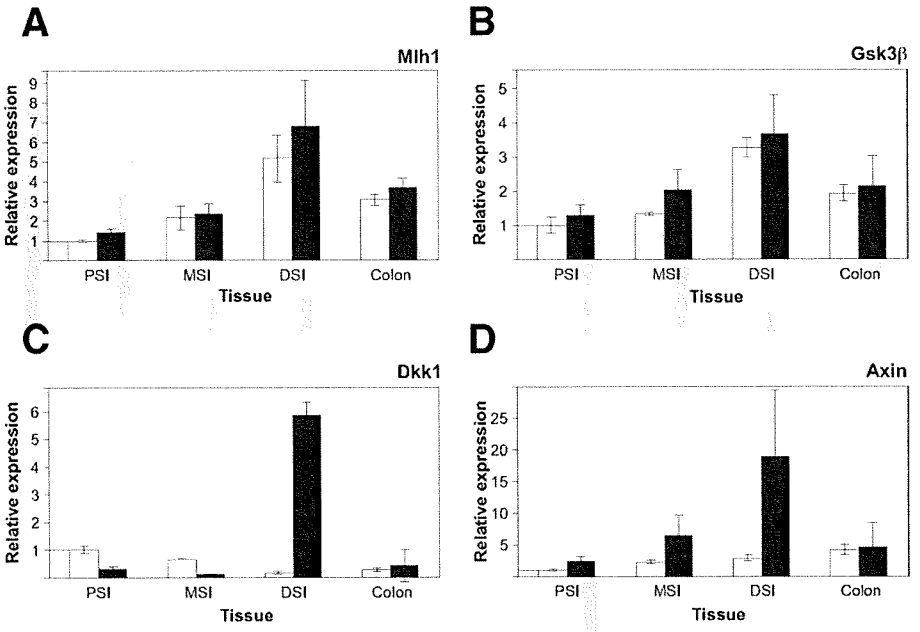

Supplementary Figure 6. Expression analysis of Wnt signaling cascade genes in normal mucosa of *A33*^{Dnmt3a} and *A33*^{wt} mice. qPCR analysis of *Mlh-1* (*A*), *Gsk-3b* (*B*), *Dkk-1* (*C*), and *Axin2/Conductin* (*D*) expression in isolated IECs from the proximal (PSI), middle (MSI), distal small intestine (DSI), and colon of *A33*^{wt} (open bars) and *A33*^{Dnmt3a} mice (filled bars). Data were normalized against expression of the house-keeping gene *Gapdh* and expressed as a multiple of the expression level in the PSI of wild-type mice. Mean values ± SD; $n = 3$.

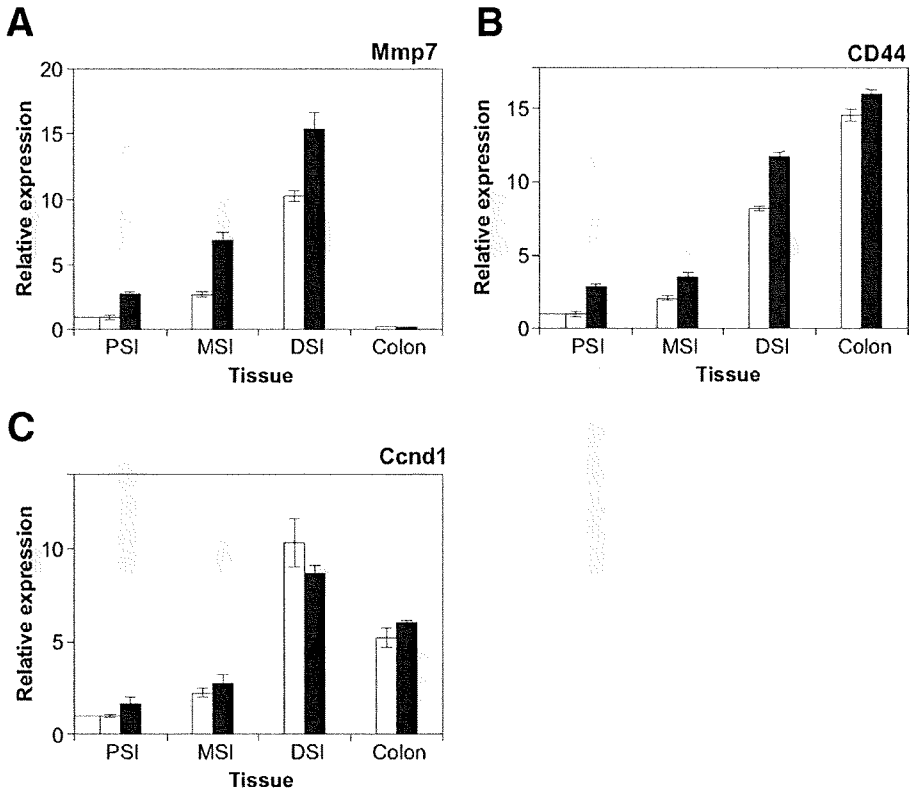

Supplementary Figure 7. Gene expression analysis in normal mucosa of $A33^{Dnmt3a}$ and $A33^{wt}$ mice. qPCR analysis for *Mmp-7* (*A*), *CD44* (*B*), and *Cyclin D1* (*C*) in IECs extracted from the proximal (PSI), middle (MSI), distal small intestine (DSI), and colons of $A33^{wt}$ (open bars) and $A33^{Dnmt3a}$ mice (filled bars). Data were normalized against expression of the house-keeping gene *Gapdh* and expressed as multiples of the expression level in the PSI of wild-type mice. Mean values ± SD; $n = 3$.

Supplementary Table 2. Nucleotide Sequence for Primers Used for Methylation-Sensitive PCR (MSP) and Bisulfite Sequencing

Gene	Amplicon	Sense primer	Antisense primer
Sfrp1	MSP1(M)	5′-TAGGTGTAGTAGTTCGTAGTTCGTC	5′-AATCCTCCGCTACAACAAATCGCCG
	MSP1(U)	5′-TAAGTAGGTGTAGTAGTTTGTAGTTTGTT	5′-TAAAATCCTCCACTACAACAAATCACCA
	MSP2(M)	5′-GTAAATCGATTTTTTTGGTCGGCGC	5′-CGAATACGCGATATACGAATAACCG
	MSP2(U)	5′-TTTAGTAAATTGATTTTTTTGGTTGGTGT	5′-AACTCAAATACACAATATACAAATAACCA
	MSP3(M)	5′-TGAAGGTAGCGTGGGTAGTTTCGAC	5′-GAACCCGCGACCAACAAAACGACG
	MSP3(U)	5′-GTGTGAAGGTAGTGTGGGTAGTTTTGAT	5′-ACCAAACCCACAACCAACAAAACAACA
Sfrp2	MSP1(M)	5′-GGTCGGAGTTTTTCGGAGTTGCGC	5′-GTAAAAACTCTAAACAACGAACGACG
	MSP1(U)	5′-TTGGGTTGGAGTTTTTTGGAGTTGTGT	5′-CTCATAAAAACTCTAAACAACAAACAACA
	MSP2(M)	5′-TAAGGTAGTTAGTTCGGTTTTACGC	5′-AATTACCTTACAAACAAACAAACGCG
	MSP2(U)	5′-TTGTAAGGTAGTTAGTTTGGTTTTATGT	5′-AATAATTACCTTACAAACAAACAAACACA
	MSP3(M)	5′-CGTTTTTCGGGGGTCGTTAGTTTAC	5′-CGCTTATAAAAAAAATCGAACTAACCG
	MSP3(U)	5′-TTTTTGTTTTTTGGGGGTTGTTAGTTTAT	5′-CTACACTTATAAAAAAAATCAAACTAACCA
Sfrp5	MSP1(M)	5′-TAGGGAATATTTTAGTCGGGGCGTAC	5′-CGAACAACAACGCCAATACGACCG
	MSP1(U)	5′-TTTTAGGGAATATTTTAGTTGGGGTGTAT	5′-CCCCAAACAACAACACCAATACAACCA
	MSP2(M)	5′-TTTTTTTAGGTTCGTTAATTCGGGGC	5′-CTCCGCTACCGAAATAATCCAAACG
	MSP2(U)	5′-GGTTTTTTTTTAGGTTTGTTAATTTGGGGT	5′-CACTCCACTACCAAAATAATCCAAACA
	MSP3(M)	5′-GGTAGGTCGAGTCGTTGTACGGTC	5′-TCCAACAAATTAAACAACCGCATACG
	MSP3(U)	5′-GTTGGTAGGTTGAGTTGTTGTATGGTT	5′-TACTCCAACAAATTAAACAACCACATACA
	Bisulfite sequencing	5′-GTGGTGGGAGGCGTTTGGATTATTT	5′-CTTATAACCCACCGTATAACAAAAC
Apc	MSP(M)	5′-GAGTGTGGTTGTCGGAAATTCGGTC	5′-CCTTCCTCAACGATAACCGACTACG
	MSP(U)	5′-TGGAGTGTGGTTGTTGGAAATTTGGTT	5′-CACCTTCCTCAACAATAACCAACTACA
	Bisulfite sequencing	5′-TATYGTAGAGGTAGGGTATAGGTTGTT	5′-TAAAAAACRCTAAAAAAACCACTCCTCA
Igf/2H19	Bisulfite sequencing 1	5′-GTTTGTTGAATTAGTTGTGGGGTTTATA	5′-TAAAAAAAAAAACTCAATCAATTACAATCC
	Bisulfite sequencing 2	5′-ATTAGTTAGTGTGGTTTATTATAGGAAG	5′-AACCATTCCAAAAATACACACATCTTA
	Bisulfite sequencing 3	5′-TTAGAGAATTTGATTTATTTTTTATATAGTT	5′-CCTAAAATACTCAAAACTTTATCACAAC

Oncogene (2009) 28, 2643–2653

www.nature.com/onc

ORIGINAL ARTICLE

CHFR, a potential tumor suppressor, downregulates interleukin-8 through the inhibition of NF-κB

L Kashima[1], M Toyota[1,2], H Mita[1], H Suzuki[1,2], M Idogawa[1], K Ogi[1], Y Sasaki[1] and T Tokino[1]

[1]*Department of Molecular Biology, Cancer Research Institute, Sapporo Medical University, Sapporo, Japan and* [2]*First Department of Internal Medicine, Sapporo Medical University, Sapporo, Japan*

The mitotic checkpoint gene *CHFR* (checkpoint with forkhead and ring finger domains) is silenced in various human cancers by promoter hypermethylation, suggesting that CHFR is a tumor suppressor. Here, we show that CHFR functions as a negative regulator of the nuclear factor-κB (NF-κB) pathway. Expression of CHFR inhibited NF-κB reporter activity, whereas knockdown of CHFR activated reporter activity. These activities are independent of its RING finger domain. Furthermore, we found that CHFR physically interacts with p65 in cells. Electrophoretic mobility shift assays (EMSAs) and ELISA-based NF-κB-binding assays showed that CHFR negatively regulated transcriptional activity of p65. In addition, our data show that interleukin (IL)-8 is significantly downregulated by CHFR, and that the migration of human endothelial cells is suppressed in culture medium conditioned from CHFR-expressing cancer cells. Using a xenograft model, we show that neovascularization is suppressed by adenovirus-mediated transfer of CHFR. These results indicate that expression of CHFR markedly reduces the expression of IL-8 through the inhibition of NF-κB. As the NF-κB signaling pathway plays a critical role in the development and progression of cancer, our findings show the functional relationship between epigenetic alteration and inflammation/angiogenesis in human cancer cells, thereby showing several potential targets for therapeutic intervention.
Oncogene (2009) **28,** 2643–2653; doi:10.1038/onc.2009.123; published online 18 May 2009

Keywords: CHFR; NF-κB; IL-8; tumor suppressor; angiogenesis

Introduction

The *CHFR* (checkpoint with forkhead and ring finger domains) gene is inactivated by promoter hypermethylation in various types of human malignancies, suggesting that the CHFR protein functions as a tumor suppressor (Privette and Petty, 2008). Furthermore, earlier studies have shown that *Chfr* knockout mice were cancer-prone, develop spontaneous tumors and have increased skin tumors after treatment with DMBA. The CHFR protein contains two conserved domains (that is, the forkhead-associated (FHA) domain and the RING finger domain) that have been identified in many different species. Originally, CHFR was believed to mediate a delay in early prophase in response to microtubule stress (Scolnick and Halazonetis, 2000). The RING finger domain is commonly found in E3 ligase proteins and is thought to influence substrate specificity during ubiquitination reactions (Jackson *et al.*, 2000). Recent studies have reported that CHFR functions as an E3 ligase in the polyubiqutination of Aurora A and PLK1 (Kang *et al.*, 2002, 2004; Yu *et al.*, 2005), resulting in the degradation of these proteins. In addition, Aurora A accumulation and increased chromosomal instability were observed in MEFs derived from *Chfr*-deficient mice (Yu *et al.*, 2005).

As a result of alternative splicing, many types of cancer cells express a CHFR variant that lacks the N-terminal FHA domain (ΔFHA-CHFR). The ΔFHA-CHFR variant acts as a *trans*-dominant inhibitor of full-length CHFR (Scolnick and Halazonetis, 2000; Toyota *et al.*, 2003). FHA domains were first identified in forkhead-type transcription factors, but are now known to exist in various proteins (Hofmann and Bucher, 1995). Many FHA-containing proteins play important roles in the regulation of DNA repair, the cell cycle and apoptosis (Durocher and Jackson, 2002). More than 200 other FHA-containing proteins have also been identified; however, the functions of many of these proteins remain unknown.

The tumor-suppressing function of CHFR is thought to be mediated by checkpoint regulation as an E3 ligase through the RING finger domain. However, very little work has focused on function of the FHA domain by interactions with multiple transcriptional regulators. Recently, decreased CHFR expression in breast cancer cells was found to result in phenotypes associated with malignant progression, including amplified anchorage-independent colony formation, increased motility and enhanced invasiveness (Privette *et al.*, 2007). However, the mechanisms underlying the effects of CHFR on the motility and invasiveness of cancer cells are poorly understood. Recently, Fukuda *et al.* (2008) reported that the anti-proliferative effects of CHFR depend on

Correspondence: Professor T Tokino, Department of Molecular Biology, Sapporo Medical University, Cancer Research Institute, S-1, W-17, Chuo-ku, Hokkaido, Sapporo 060-8556, Japan.
E-mail: tokino@sapmed.ac.jp
Received 21 November 2008; revised 31 March 2009; accepted 21 April 2009; published online 18 May 2009

the FHA domain, rather than on the E3 ligase activity mediated by the RING finger domain (Fukuda *et al.*, 2008).

We carried out cDNA microarray analysis to determine whether CHFR plays a role in transcriptional regulation. Our results show that CHFR downregulates the pro-inflammatory chemokine, interleukin-8 (IL-8), a target of nuclear factor-κB (NF-κB). In addition, CHFR interacts with RelA (p65) to suppress NF-κB signaling. Using a xenograft model of human cancer, we show that neovascularization is suppressed by adenovirus-mediated transfer of CHFR. Our data identify a novel mechanism by which inactivation of the tumor suppressor, CHFR, results in cancer progression.

Results

CHFR downregulates NF-κB-dependent transcription

To address the effects of CHFR on gene regulation, we carried out a cDNA microarray analysis (using Affymetrix GeneChips, Affymetrix, Santa Clara, CA, USA) of HCT116 cells that had been infected with recombinant adenoviruses expressing either CHFR (Ad-CHFR) or Ad-EGFP (Figure 1a). We chose to use HCT116 cells because the *CHFR* gene is epigenetically silenced in this colorectal cancer cell line (Toyota *et al.*, 2003). The expression of several NF-κB target genes was substantially downregulated in CHFR-infected cells. To validate the results of our global gene expression analysis, we examined the reduction of representative NF-κB targets using real-time RT–PCR. The real-time RT–PCR analysis showed that expression of several NF-κB target genes, particularly *IL8*, was considerably lower in HCT116 cells after infection with Ad-CHFR than after infection with Ad-EGFP (Figure 1b). It is noteworthy that the reduction in expression level varied among the NF-κB target genes. Several different *cis*-acting elements, together with a binding site for the inducible NF-κB, have been identified within the regulatory regions of NF-κB target genes. The varying effects of CHFR most likely reflect differences in the mechanisms of regulation for each of the NF-κB target genes.

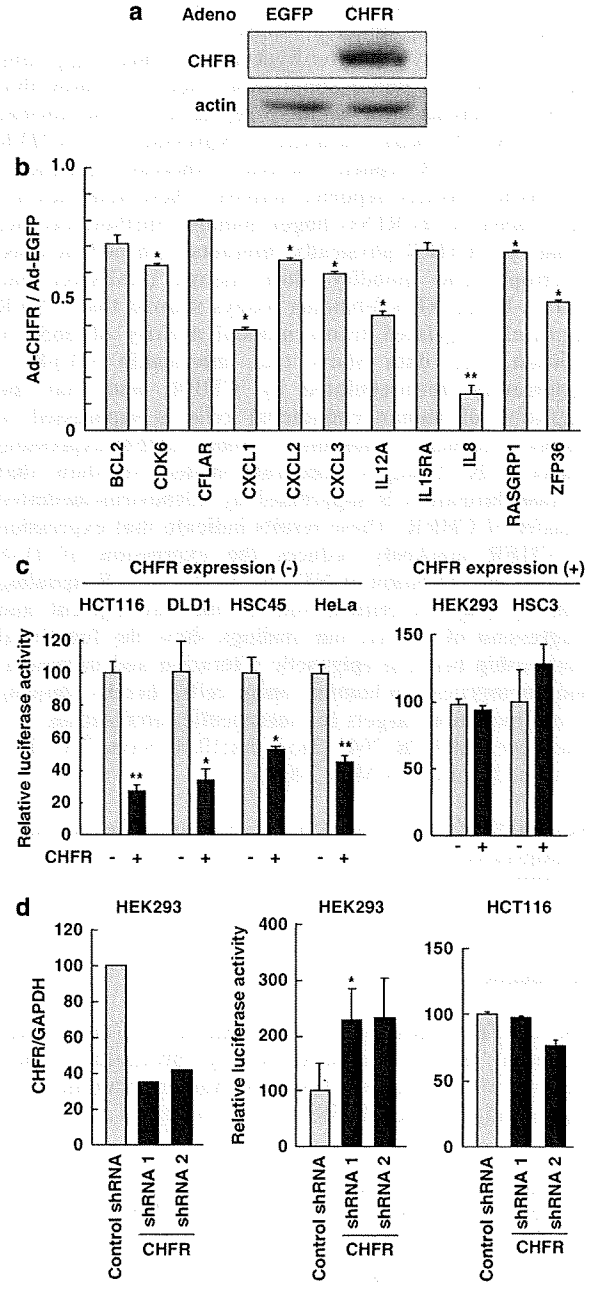

Figure 1 NF-κB-dependent transcription is downregulated by CHFR. (**a**) HCT116 cells were infected with an adenovirus expressing EGFP (Ad-EGFP) or CHFR (Ad-CHFR). Immunoblot analysis was carried out using an anti-CHFR antibody. (**b**) HCT116 cells were infected with Ad-CHFR or Ad-EGFP. Total RNA from the infected cells was subjected to real-time RT–PCR analysis using the TaqMan Gene Expression Assay. Putative target gene signals were normalized to those of GAPDH mRNA. Cells infected with Ad-EGFP served as controls and the Ad-CHFR/Ad-EGFP ratio is shown on the *y*-axis. Experiments were carried out in triplicate. Means and standard deviations are indicated by bars and brackets, respectively. $*P<0.05$; $**P<0.01$ relative to mock Ad-EGFP-infected samples. (**c**) Cancer cells lacking the CHFR expression (HCT116, DLD1, HSC45 and HeLa), and CHFR-expressing cells (HEK293 and HSC3) were transfected with an NF-κB firefly luciferase reporter along with a Flag-CHFR expression vector (+) or an empty vector (−). Luciferase activity was determined by using a dual luciferase assay system. (**d**) HEK293 cells were transfected with an shRNA expression vector (either CHFR-shRNA1 or CHFR-shRNA2) or with an empty vector (Control-shRNA) and were subjected to real-time RT–PCR analysis. CHFR mRNA signals were normalized to those of GAPDH mRNA. HEK293 and HCT116 cells were transfected with an NF-κB luciferase reporter and with an shRNA expression vector or an empty vector. Luciferase activity was determined by using a dual luciferase assay system. Experiments were carried out in triplicate. Means and standard deviations are indicated by bars and brackets, respectively. $*P<0.05$; $**P<0.01$ relative to mock samples transfected with empty vectors.

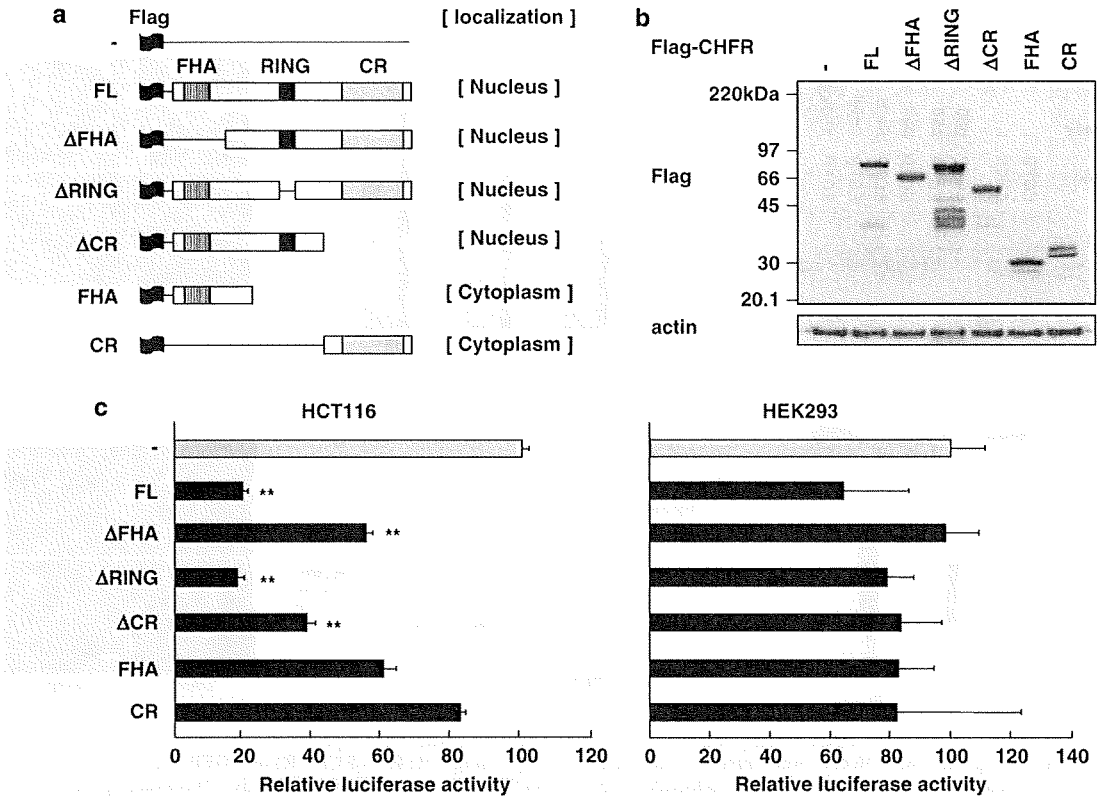

Figure 2 NF-κB activity is suppressed by CHFR in a RING-domain-independent manner. (**a**) CHFR deletion constructs used in this study. The structural domains of CHFR and the intracellular localization of each mutant are shown (also see Supplementary Figure S2). FL, full-length CHFR [Flag-CHFR, amino acids (aa) 1–652]; ΔFHA, delta forkhead-associated domain (aa 149–652); ΔRING, delta ring finger domain (deleted aa 291–334); ΔCR, delta cysteine-rich domain (aa 1–416); FHA, (aa 1–186); CR, (aa 418–652). (**b**) HCT116 cells were transfected with Flag-CHFR deletion constructs or with an empty vector (pCMV-tag2B, indicated by '–'). Immunoblot analysis was carried out using anti-Flag and anti-actin antibodies. (**c**) HCT116 and HEK293 cells were transfected with an NF-κB luciferase reporter construct, along with a Flag-CHFR deletion construct or with an empty vector (–). Luciferase activity was determined using a dual luciferase assay system. Experiments were carried out in triplicate. Means and standard deviations are indicated by bars and brackets, respectively. $^{**}P<0.01$ relative to mock samples transfected with empty vectors.

To examine the role of CHFR in regulation of the NF-κB signaling pathway, we carried out reporter assays using a luciferase reporter (pNF-κB-Luc). CHFR-expressing cells (HEK293 and HSC3) and cancer cells lacking CHFR expression (HCT116, DLD1, HSC45 and HeLa) were co-transfected with pNF-κB-Luc and either a CHFR-expressing plasmid or an empty plasmid. The luciferase activity was lower in the CHFR-negative cells co-transfected with the CHFR expression vector (Figure 1c, left panel). In contrast, transfection of CHFR had little effect on NF-κB reporter activity in the CHFR-expressing cells (Figure 1c, right panel).

We next examined whether knockdown of CHFR would trigger NF-κB activity in human cells. Transfection of HEK293 cells with an shRNA expression vector (either CHFR-shRNA1 or CHFR-shRNA2, see Materials and methods) decreased CHFR expression by <40% (Figure 1d, left panel). We then co-transfected HEK293 and HCT116 cells with the NF-κB reporter plasmid, and either with an shRNA expression vector or with an empty vector (pSilencer). Knockdown of CHFR increased NF-κB reporter activity in HEK293 cells (Figure 1d, middle panel). Introduction of the CHFR-shRNAs into HCT116 cells, which lack CHFR expression, did not affect NF-κB reporter activity (Figure 1d, right), indicating that these outcomes were not due to off-target effects. These results suggest that CHFR downregulates basal NF-κB transcriptional activity.

CHFR suppresses NF-κB activity in a RING domain-independent manner

The CHFR protein contains FHA and RING domains, which contribute to this protein's checkpoint activity. To identify the specific domains involved in the regulation of NF-κB activity, we transfected HCT116 and HEK293 cells with the NF-κB reporter plasmid and various deletion constructs of CHFR (Figure 2a). Expression of each CHFR deletion construct was similar (Figure 2b). Interestingly, the activities of ΔRING-CHFR and full-CHFR suppressed NF-κB to similar extents in HCT116 cells (Figure 2c, left panel). However, the other CHFR deletion constructs partially restored the suppressed NF-κB activity. In HEK293

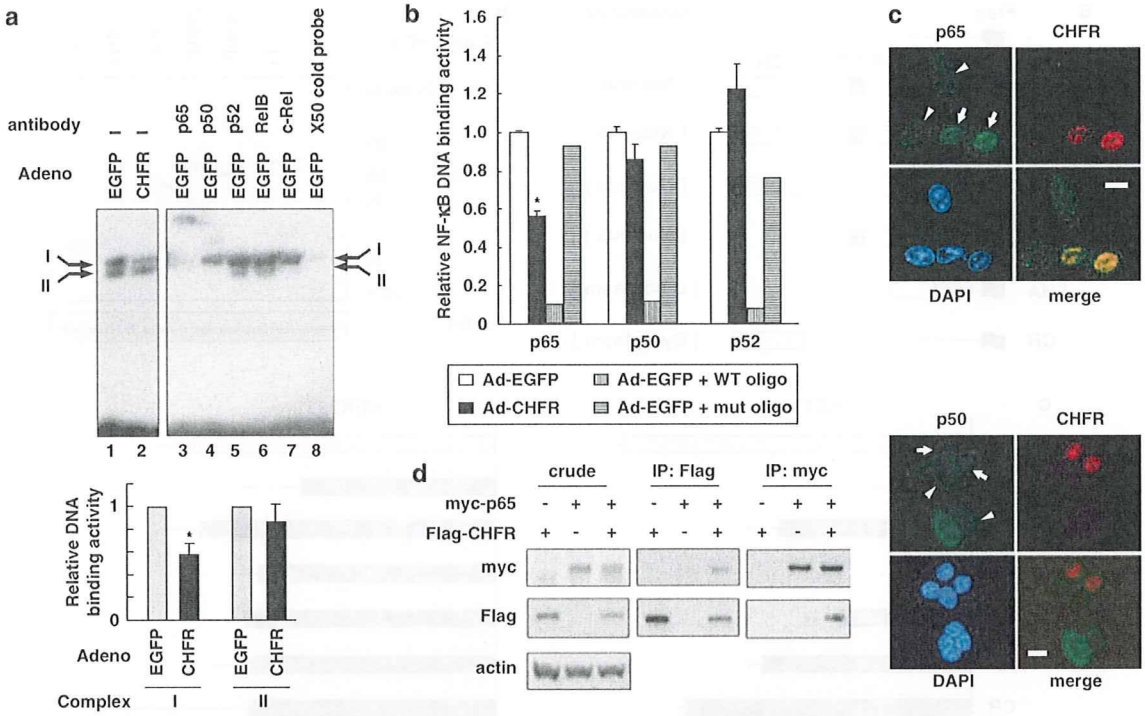

Figure 3 CHFR suppresses the DNA-binding activity of NF-κB by interacting with NF-κB p65 in the nucleus. (**a**) EMSAs to assess the NF-κB-binding site. HCT116 cells were infected with adenovirus expressing CHFR (Ad-CHFR) or EGFP (Ad-EGFP). Nuclear extracts were incubated with a ^{32}P-labeled oligonucleotide probe (5′-AGTTGAGGGGACTTTCCCAGGC-3′) containing an NF-κB-binding site (underlined), and complexes were resolved in a 4% nondenaturing polyacrylamide gel. Supershift analysis (right) was carried out by preincubation with antibodies against various NF-κB/Rel subunits. Arrows indicate DNA–protein complexes I and II (top). Complex I represents p65 homodimers and complex II contains p65/p50 and p65/c-Rel heterodimers. Densitometry and quantification of EMSAs (bottom). (**b**) Nuclear extracts from HCT116 cells infected with Ad-CHFR or Ad-EGFP were monitored using ELISA-based colorimetric assays. Wild-type consensus NF-κB (WT oligo) and mutated oligonucleotides (mut oligo) were used in competition experiments. Experiments were carried out in triplicate. Means and standard deviations are indicated by bars and brackets, respectively. $*P<0.05$ relative to mock Ad-EGFP-infected samples. (**c**) Immunofluorescence analysis of HCT116 cells transfected with Flag-CHFR expression plasmids. Cells were fixed, stained with antibodies to the Flag epitope (red) and to p65 or p50 (green), incubated with the appropriate secondary antibodies and analysed using double immunofluorescence assays. Colocalization of p65 and CHFR in the nuclei (yellow coloration in merged images). Nuclei were detected through DAPI staining (blue). Cells expressing and not expressing Flag-CHFR are indicated by arrows and arrowheads, respectively. Bar = 10 μm. (**d**) HCT116 cells were transfected with Flag-CHFR and myc-p65, as indicated. Equal amounts of protein extracts were pre-cleaned with protein G-Sepharose (Amersham Biosciences), incubated with 4 μg of anti-Flag (IP: Flag, middle column) or anti-myc antibodies (IP: myc, right column) and with 30 μl of 25% protein G-Sepharose and incubated at 4 °C. The immunoprecipitates were washed five times in the HBST buffer and then boiled in the 1 × SDS sample buffer. Samples were separated in a 10% SDS–PAGE gel, transferred to an Immobilon-P membrane (Millipore, Billerica, MA, USA), probed with antibodies specific to the myc- (top row) or Flag-(middle row) epitopes and visualized with enhanced chemiluminescence (Amersham Bioscience).

cells that express CHFR, none of the CHFR deletion mutants had significant effects on NF-κB reporter activity (Figure 2c, right panel). These results indicate that CHFR does not require the RING domain for suppression of NF-κB-dependent transcription.

CHFR suppresses the DNA-binding activity of NF-κB by interacting with p65 in the nucleus

We carried out EMSAs to determine whether CHFR inhibits the sequence-specific DNA-binding activity of the NF-κB protein complex. First, we infected HCT116 cells with Ad-CHFR or Ad-EGFP, and then incubated nuclear extracts from these cells with a radiolabeled oligonucleotide probe containing an NF-κB DNA-binding site. Two DNA–protein complexes appeared on the gel, which we designated as NF-κB DNA-binding complex I (upper band) and II (lower band). Complex I was significantly reduced in Ad-CHFR-infected cells (Figure 3a, lanes 1 and 2 and lower graph). The NF-κB transcription factor is a dimeric complex consisting of Rel/NF-κB family proteins, such as RelA (p65), RelB, c-Rel, NFKB1 (p105/p50) and NFKB2 (p100/p52). Supershift analyses were carried out using specific antibodies against each component of NF-κB to determine which components contribute to the reduction of DNA–protein binding by CHFR. An antibody specific to the p65 subunit shifted the mobility of the complex I and complex II bands (Figure 3a, lane 3), whereas antibodies against p50 and c-Rel supershifted only complex II (Figure 3a, lanes 4 and 7). In addition, antibodies against p52 and RelB shifted the mobility of

these two complexes slightly (Figure 3a, lanes 5 and 6), indicating that complex I is a p65 homodimer and complex II is mainly composed of p65/p50 and p65/-c-Rel heterodimers, which is consistent with earlier reports (Sathe *et al.*, 2004; Wan *et al.*, 2007). Therefore, CHFR mainly affected the DNA-binding activity of the p65 homodimer (Figure 3a, lane 2, complex I). We further validated the role of CHFR in suppression of NF-κB activity using the TransAM NFκB Family Transcription Factor Assay kit (Active Motif), which allows the DNA-binding activity of each subunit of NF-κB transcription factors to be quantitatively analysed. Lower levels of activated p65 were observed in nuclear extracts from Ad-CHFR-infected HCT116 cells than in Ad-EGFP-infected HCT116 cells (Figure 3b). RelB and c-Rel activities were not detectable (date not shown). The DNA-binding activity of p65 was competed by wild-type oligonucleotides, but not by mutant oligonucleotides (Figure 3b). These results suggest that the DNA-binding activity of p65 homodimer is suppressed by CHFR expression.

We next carried out an NF-κB luciferase assay in the presence of tumor necrosis factor-α (TNF-α) or IL-1β to examine the role of CHFR under the NF-κB-stimulated conditions. The luciferase activity did not increase significantly in response to TNF-α or recombinant IL-1β stimulation in HCT116 cells (Supplementary Figure S1). Furthermore, EMSAs with nuclear extracts prepared from HCT116 cells showed that NF-κB transcription factors had already obtained sequence-specific DNA-binding activity in the absence of any stimulation (Figure 3a, lane 1). These results suggest that NF-κB is constitutively activated in HCT116 cells, consistent with the reports that NF-κB is constitutively activated in various other cancer cell lines, including the colon cancer cell lines HCT116, HT29, HCT15, LoVo, and SW480 (Rakitina *et al.*, 2003; Williams *et al.*, 2008).

To determine whether the CHFR protein colocalizes with the p65 protein in cells, we transfected HCT116 cells with a Flag-CHFR expression vector and carried out immunostaining using antibodies against p65 and Flag. Endogenous p65 appeared to be colocalized with CHFR in the nucleus of CHFR-transfected HCT116 cells, whereas p65 localized in the cytoplasm as well as in the nucleus of CHFR-negative HCT116 cells (Figure 3c, top panels). In contrast, endogenous p50 did not appear to colocalize with CHFR in CHFR-transfected HCT116 cells (Figure 3c, bottom panels). Similar data were obtained in HeLa cells (data not shown). In general, the IκBs retain NF-κB in the cytoplasm by masking the nuclear localization sequence embedded within the REL homology domain (Karin *et al.*, 2002). p65 is translocated into the nucleus when it is liberated from IκBα after activation. Our results suggest that CHFR cannot physically associate with the cytoplasmic p65 (in the NF-κB/IκB complex), but can associate with the nuclear p65 (liberated from IκBα).

We subsequently carried out a co-immunoprecipitation assay to determine whether CHFR interacts with p65. HCT116 cells were co-transfected with plasmids expressing Flag-tagged CHFR and myc-tagged p65. Protein extracts were immunoprecipitated with anti-Flag or anti-myc antibodies and subjected to immunoblotting analysis. The results showed that Flag-CHFR associates with myc-p65 in HCT116 cells (Figure 3d). Similar data were obtained from a co-immunoprecipitation assay using myc-CHFR and Flag-p65 constructs (data not shown). Furthermore, an immunocytochemical analysis showed that the CHFR deletion constructs, FHA-CHFR and CR-CHFR, were localized in the cytoplasm (Supplementary Figure S2), where p65 is retained by IκBα. FHA-CHFR and CR-CHFR did not associate with myc-p65 (data not shown) and did not significantly suppress NF-κB-dependent transcription in HCT116 cells (Figure 2c). These findings strongly suggest that CHFR can interact with p65 liberated from IκBα in the nucleus, thereby reducing sequence-specific DNA-binding activity and suppressing NF-κB-dependent transcription.

NF-κB-dependent transcription of IL-8 is downregulated by CHFR

Expression of *IL8*, a well-known NF-κB target gene (Matsusaka *et al.*, 1993), was significantly downregulated by CHFR (Figure 1b). The transcriptional events required for activation of the *IL8* promoter have been extensively studied. In particular, the transcription factors AP-1, NF-IL6 and NF-κB play central roles in the modulation of IL-8 expression. We carried out an *IL8* promoter–reporter assay to identify regulatory elements within the *IL8* gene necessary for its down-regulation by CHFR. Single binding sites for the transcription factors, AP-1, NF-IL6 and NF-κB, have been identified earlier in the *IL8* promoter (Yasumoto *et al.*, 1992). We first cloned a 196-base pair (bp) region of the *IL8* promoter containing these known transcription factor-binding elements (Figure 4a) and inserted the 196-bp fragment and a deleted construct upstream of the luciferase reporter gene (Figure 4b). These constructs were then used in reporter assays. HCT116 cells were transiently co-transfected with a reporter plasmid and a CHFR expression vector. A luciferase reporter containing a consensus p53-binding site (pGL-p53CBS) was used as a control plasmid (Sasaki *et al.*, 2002). Figure 4b showed that (1) the pGL-IL8-54 reporter construct encompassing nucleotides −54 to +44 of the IL8 gene relative to the transcription start site conferred little luciferase activity; (2) pGL-IL8-152 luciferase activity was significantly reduced by co-transfection of the CHFR expression vector; and (3) CHFR expression did not influence the luciferase activity of pGL-p53CBS. Altogether, these data suggest that nucleotides −152 to −55 of the promoter, which contain the NF-κB response site, are important for the CHFR-mediated transcriptional suppression of IL-8.

We then examined IL-8 protein expression in cell culture medium with an ELISA to determine whether the reduction in IL-8 mRNA was accompanied by decreased protein secretion. Significantly less IL-8 protein was secreted from CHFR-infected HCT116 cells (Figure 4c).

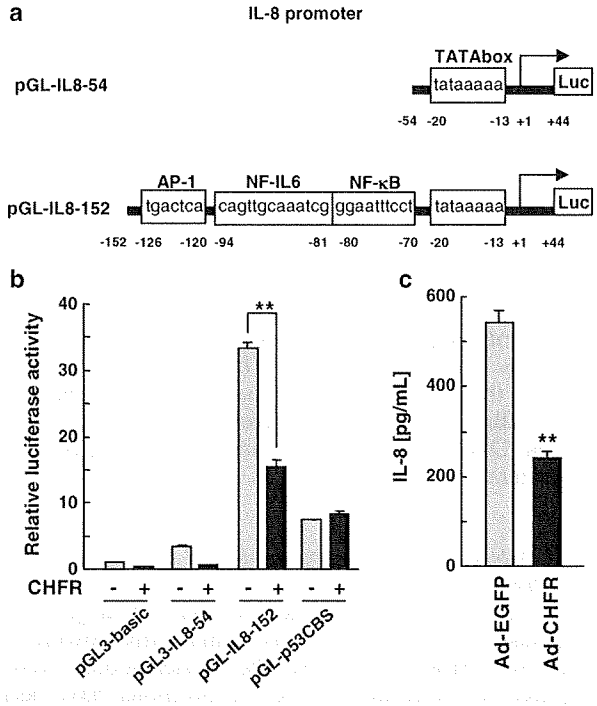

Figure 4 NF-κB-dependent transcription of IL-8 is downregulated by CHFR. (**a**) The IL-8 promoter–reporter constructs. Fragments containing 5′-flanking regions of the IL-8 gene were subcloned upstream of a luciferase reporter gene in the pGL3-Basic vector. The transcriptional start site was defined as +1. The TATA box, and the NF-κB, NF-IL6 and AP-1 binding sites are located at −13, −70, −81 and −120, respectively. (**b**) Luciferase assays to assess the IL-8 promoter activity. HCT116 cells were co-transfected with each of the reporter plasmids and the CHFR expression vector. Experiments were carried out in triplicate. Means and standard deviations are indicated by bars and brackets, respectively. $^{**}P<0.01$ relative to mock samples transfected with empty vectors. (**c**) Conditioned media from Ad-CHFR (CHFR-CM)- and Ad-EGFP (EGFP-CM)-infected HCT116 cells were collected. The conditioned media were analysed using an ELISA kit specific to human IL-8 (R&D Systems). Experiments were carried out in triplicate. Means and standard deviations are indicated by bars and brackets, respectively. $^{**}P<0.01$ relative to mock Ad-EGFP-infected samples.

CHFR inhibits migration of HUVECs through the regulation of IL-8 expression

IL-8 induces migration of endothelial cells and is involved in the regulation of pathological angiogenesis, tumor growth and metastasis (Koch *et al.*, 1992; Yuan *et al.*, 2005). As CHFR suppresses IL-8 expression, we examined whether it also inhibits the motility of endothelial cells. To this end, we carried out a wound-healing assay to assess the effects of CHFR on the motility of HUVECs. Conditioned media from Ad-CHFR-infected HCT116 cells (CHFR-CM) significantly decreased HUVECs motility compared with those from Ad-EGFP-infected cells (EGFP-CM; Figure 5a, top row). We then inhibited IL-8 function using an IL-8-neutralizing antibody, MAB208, to investigate its role in CHFR-mediated inhibition of cell motility. Cellular motility was inhibited by the neutralizing antibodies against IL-8 (Figure 5a, second row). Conversely, the inhibitory effects of CHFR-CM on HUVECs migration were abrogated by the addition of recombinant IL-8 (Figure 5a, third row). These data suggest that CHFR inhibits HUVECs migration through the downregulation of IL-8.

We then carried out *in vitro* assays to examine the role of CHFR in angiogenesis. The effects of CHFR on the chemotactic migration of HUVECs were evaluated using the Matrigel migration assay. The number of HUVECs that migrated from the upper to the lower chamber was significantly lower in HUVECs cultured with CHFR-CM than in HUVECs cultured with EGFP-CM (Figure 5b). When neutralization antibodies against IL-8 were added, the migration of the cells cultured with EGFP-CM was similar to that of the cells cultured with CHFR-CM (Figure 5b). These results strongly suggest that CHFR inhibits the migration of HUVECs through downregulation of IL-8.

CHFR represses angiogenesis in a xenograft model of human cancer

To further examine the role of CHFR in the regulation of angiogenesis and tumor growth *in vivo*, we conducted xenograft studies in immunocompromised nude mice. Animals were divided into two experimental groups. The first cohort was subcutaneously injected with HCT116 cells and received intratumoral injections of Ad-CHFR every 1 days. The second cohort was subcutaneously injected with HCT116 cells and received intratumoral injections of Ad-EGFP (as a control). Animals were monitored for subcutaneous tumor formation and tumor growth rates were determined. Ad-CHFR injection slightly inhibited tumor growth and *IL8* expression in experimental animals (data not shown). We speculated that the decrease in tumor growth after Ad-CHFR administration reflected an impairment of angiogenesis. To test this hypothesis, we histochemically evaluated tumor-associated blood vessels for the presence of CD31, an endothelial cell surface marker, which should attenuated vascularization in tumors injected with Ad-CHFR (Figure 6a). These results suggest that CHFR-mediated inhibition of angiogenesis and tumorigenesis requires IL-8 down-regulation through the inhibition of NF-κB signaling.

Discussion

We have shown for the first time that CHFR is involved in gene regulation. CHFR suppressed IL-8 transcription by inhibiting NF-κB in human cancer cells, which subsequently decreased angiogenesis *in vivo* and the migration of human endothelial cells *in vitro*. These findings show that CHFR functions as a tumor suppressor through the NF-κB signal pathway (Figure 6b). Mitotic stress activates NF-κB (Rosette and Karin, 1995), whereas inhibition of NF-κB results in mitotic arrest (Cude *et al.*, 2007). Thus, CHFR may act as an antephase checkpoint, not only through

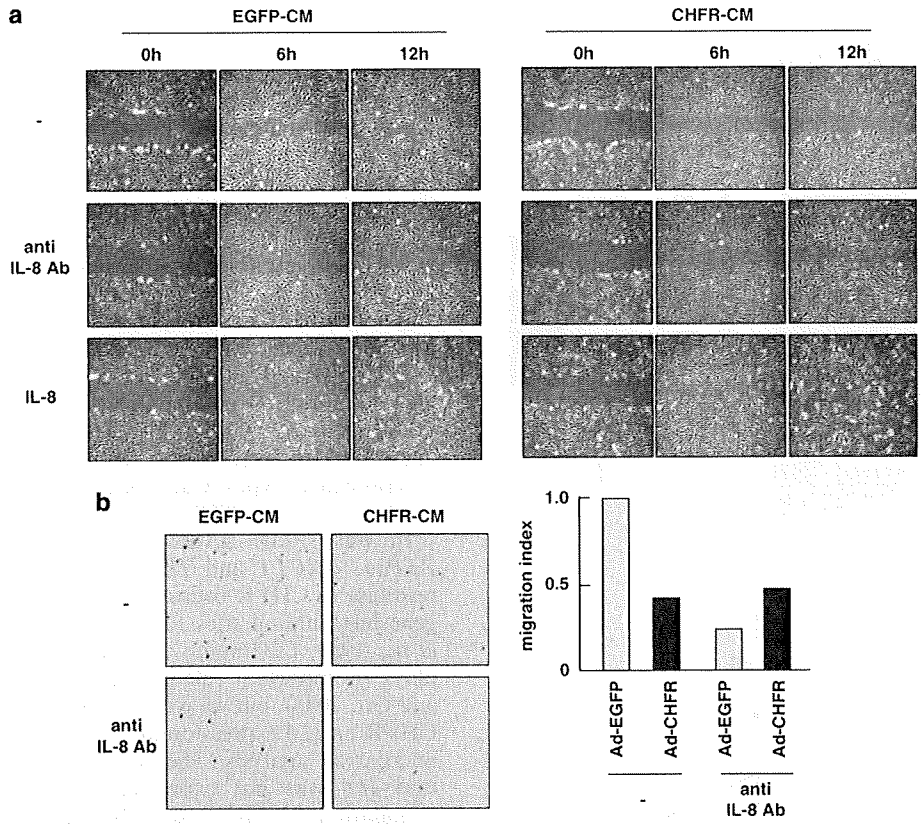

Figure 5 CHFR inhibits migration of human umbilical vein endothelial cells in an NF-κB-dependent manner through the suppression of IL-8 expression. (**a**) HCT116 cells were infected with adenovirus Ad-CHFR or with Ad-EGFP. After 32 h of incubation, the growth medium was changed to remove adenoviruses and cells were incubated for an additional 16 h. Conditioned media (CM) were collected and used in wound-healing assays. EGFP-CM and CHFR-CM refer to the conditioned media from Ad-CHFR- and Ad-EGFP-infected cells, respectively. HUVECs were grown to confluence on six-well plates and wound-healing assays were carried out using 100 μl of conditioned media in the presence or absence (−) of an anti-IL-8 antibody (400 ng/ml) or in recombinant human IL-8 (0.1 ng/ml). (**b**) Conditioned media (CM) were placed in the lower chamber in the presence or absence of an anti-IL-8 antibody (400 ng/ml). Subsequently, HUVECs were seeded onto a Matrigel-coated chamber and migration assays were carried out. EGFP-CM and CHFR-CM refer to the conditioned media from Ad-CHFR- and Ad-EGFP-infected cells, respectively. Original magnification, × 200 (left). The average number of migrating cells was determined by counting the cells under a microscope in at least five different viewing fields. The migration index was normalized to the average number of cells migrating through a control membrane (right).

ubiquitination but also through the regulation of NF-κB.

We do not know the exact molecular basis for the downregulation of NF-κB signaling in cells expressing CHFR. We propose that CHFR cannot physically interact with the p65 subunit in the NF-κB/IκB complex (the inactivated form in the cytoplasm), but can interact with the p65 subunit when it is liberated from IκBα and has translocated to the nucleus. Although nuclear localization of p65 protein is an index of NF-κB activation, an interaction between p65 and CHFR in the nucleus reduces the sequence-specific DNA-binding activity of p65. Consequently, CHFR negatively regulates transcriptional activity of the NF-κB complex. The FHA domain may be important for CHFR to inhibit the transcriptional activity of p65. In general, FHA domains are protein modules that switch signals in diverse biological pathways by monitoring the phosphorylation of threonine residues of target proteins. The FHA domain of CHFR is important for proper subnuclear localization of CHFR to promyelocytic leukemia protein bodies (Daniels *et al*., 2004). Promyelocytic leukemia transcriptionally represses NF-κB by interacting with p65 (Wu *et al*., 2003). The ΔFHA-CHFR mutant does not interact with promyelocytic leukemia, suggesting that CHFR recruitment to promyelocytic leukemia bodies requires the FHA domain and that this recruitment may be relevant to the downregulation of NF-κB. As a next step, we will attempt to clarify the molecular mechanism by which CHFR interacts with and inhibits the transcriptional activity of p65.

As recently discussed, the NF-κB signaling pathway plays a critical role in cancer development and progression. Aberrant activation of NF-κB (arising from mutation, amplification or deletion of NF-κB family members and upstream genes, or aberrant activation of upstream signaling pathways) is frequently observed in many types of human cancers. The first gene in the NF-κB family that was found to be mutated in human

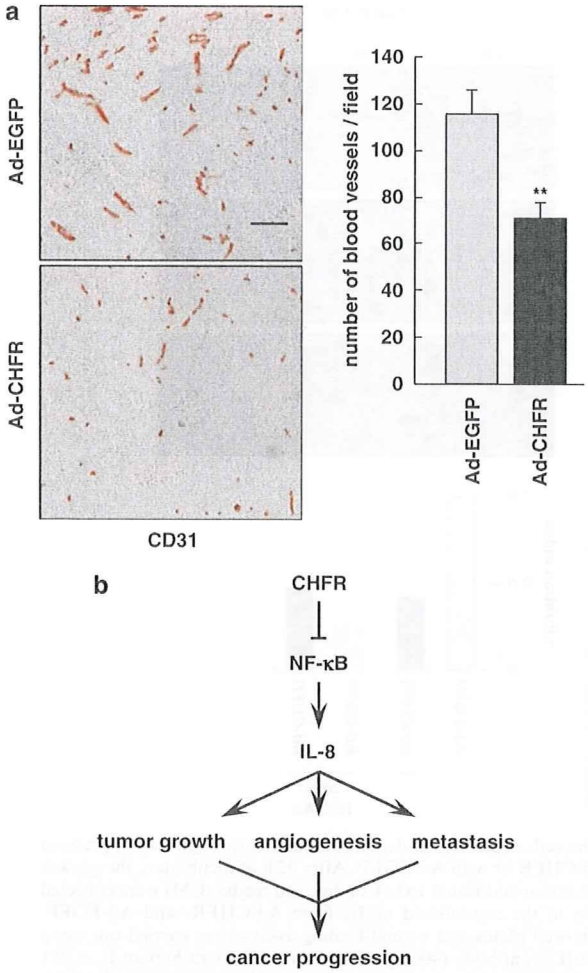

Figure 6 CHFR represses angiogenesis in a xenograft model of human cancer. (**a**) Studies were conducted in immunocompromised nude mice by resuspending 3×10^6 of HCT116 cells in 100 µl of sterile PBS and subcutaneously injecting these cells into the flanks of animals using a 21-gauge needle. A total of 3×10^8 plaque forming units (pfu) per 100 µl of adenovirus Ad-CHFR or Ad-EGFP were intratumoraly injected on days 6, 8, 10, 12, 14, 16 and 18 after tumor cell inoculation, using a 26-gauge needle. Mice were killed on day 20 after tumor cell inoculation. For immunohistochemical staining, snap-frozen sections of tumor specimens (10 µm thick) were fixed in acetone. The sections were incubated with an anti-CD31 antibody (1:20) overnight at room temperature, following which the appropriate biotinylated secondary antibody was added. After incubation with the secondary antibody, streptavidin-HRP (horseradish peroxide) was applied (BD Pharmingen) and the subsequent antibody/enzyme conjugate was developed using DAB. All sections were counterstained using hematoxylin. Tumor sections were imaged at low magnification (×4), and blood vessels density was quantified by counting the total number of CD31-positive vessels in each of two fields. For this analysis, eight tumor samples were evaluated for each experimental condition. Bar = 200 µm (left panel). Blood vessel density was determined by morphometric analysis. Values represent the averages of eight independent tumors per experimental condition. Means and standard errors are indicated by bars and brackets, respectively. $^{**}P<0.01$ relative to mock Ad-EGFP-injected samples (right panel). (**b**) Role of CHFR in tumor suppression. Our findings indicate that CHFR suppresses tumor growth and angiogenesis through the inhibition of NF-κB signaling.

lymphoid malignancies was *NFKB2* (p100). Subsequent studies showed that chromosomal rearrangements at the *NFKB2* locus occur in a variety of human lymphomas (Rayet and Gelinas, 1999). Other changes to NF-κB family proteins in cancer tissues include the amplification and mutation of *REL* (c-Rel) in leukemia and lymphomas (Rayet and Gelinas, 1999; Starczynowski *et al*., 2007); mutations in the *IKBA* (IκBα) gene and hemizygous frameshift mutations in *IKBE* (IκBε) in Hodgkin's lymphoma (Cabannes *et al*., 1999; Scolnick and Halazonetis, 2000) (Emmerich *et al*., 2003); the amplification and overexpression of the *IKBKE* (IKKε) gene, a member of the IKK family, in breast cancer cell lines and patient-derived tumors (Boehm *et al*., 2007); and the mutation or amplification of *TRAF2*, *TRAF3*, *CYLD*, *CIAP2*, *CD40*, *LTBR*, *TACI*, *NIK*, *CARD11* and other activators of the NF-κB signaling pathway in several cancer types (Campbell *et al*., 1998; Keats *et al*., 2007; Lenz *et al*., 2008).

In our study, several NF-κB target genes (*IL8*, *ZFP36*, *CXCL1* and *IL12A*) were downregulated in response to CHFR overexpression (Figure 1b). The *IL6* gene has binding sites for NF-IL6 and NF-κB (Akira *et al*., 1990; Libermann and Baltimore, 1990) and also plays an important role in tumor development (Mumm and Oft, 2008), but we were unable to detect an effect of CHFR on *IL6* expression in HCT116 cells in our cDNA microarray analysis. The RT–PCR analysis confirmed that *IL6* was not expressed or induced by TNF-α stimulation in HCT116 cells (Supplementary Figure S3a). As a control, we used HeLa cells, in which the expression and induction of *IL6* were reported earlier (Kontermann *et al*., 2008). Therefore, we concluded that *IL6* was probably silenced epigenetically or by other means in HCT116 cells. Subsequent RT–PCR experiments showed that the IL-6 expression was downregulated in response to CHFR expression both with and without TNF-α stimulation in HeLa cells (Supplementary Figure S3b). These results indicate that *IL6* is also downregulated by CHFR through inhibition of NF-κB. In contrast, a subset of NF-κB target genes (*VEGF*, *BIRC5*, *BCL10* and *CXCL5*, *6*) did not respond in the same manner (data not shown). It is possible that CHFR binds other transcription factors that are critical for transactivating a subset of the NF-κB target genes.

Clinical studies have shown that IL-8 is upregulated in several human malignances, including melanoma (Nurnberg *et al*., 1999), colon (Cuenca *et al*., 1992), stomach (Lee *et al*., 2004), non-small-cell lung (Smith *et al*., 1994) and other types of cancers. Generally, IL-8 production is linked to tumor vascularization, a metastatic phenotype and an overall poor prognosis. The tumor microenvironment and the biological activity of IL-8 in tumors may contribute to tumor progression through the regulation of angiogenesis, cancer cell growth and survival, tumor cell motion, leukocyte infiltration and the immune response.

Expression of IL-8 can be induced by various stimuli, including pro-inflammatory cytokines, bacterial products and various cellular stresses. Kunsch and Rosen (1993) reported that, unlike most other well-characterized

NF-κB-binding elements, the NF-κB site within *IL8* prefers to bind p65, p52 and c-Rel homodimers rather than to p65–p50 heterodimers and p50 homodimers (Kunsch and Rosen, 1993). Consistent with these data, we found that the NF-κB site within the *IL8* promoter is critical for transcriptional suppression by CHFR, which primarily interacts with p65 homodimers.

In this study, we have explored the functional significance of IL-8 downregulation by the tumor suppressor CHFR. Downregulation of IL-8 is necessary for CHFR-induced inhibition of human endothelial cell migration. In addition, tumor vasculature was substantially decreased in CHFR-infected tumors, as determined in a xenograft model. Taken together, our results show that frequent inactivation of CHFR may trigger NF-κB activation in human cancer cells. These observations show the functional relationship between epigenetic alteration and inflammation/angiogenesis in human cancers, and also show several potential targets for therapeutic intervention.

Materials and methods

Cell cultures

Human colorectal cancer cells (HCT116 and DLD1), human stomach cancer cells (HSC45), human oral squamous cell carcinoma cells (HSC3), human cervical carcinoma cells (HeLa), human embryonic kidney cells (HEK293) and monkey kidney cells (COS7) used in this study were purchased from the American Type Culture Collection (Manassas, VA, USA) or the Japanese Collection of Research Bioresources (Tokyo, Japan). Human umbilical vein endothelial cells (HUVECs) were purchased from Cambrex Bio Science (Walkersville, MD, USA). All cells were cultured in appropriate media as recommended by the suppliers.

Plasmids and recombinant adenoviruses

The cDNAs encoding full-length CHFR and deletion constructs (see Figure 2a) were inserted into Flag-tagged pCMV-tag2B or pCMV-tag2C vector (Stratagene, La Jolla, CA, USA). The shRNA expression vectors designed to interfere with CHFR expression (CHFR-shRNA1 (pSilencer-CHFR487) and CHFR-shRNA2 (pSilencer-CHFR500)) were described earlier (Ogi *et al*., 2005). The pcDNA3-Flag-p65 construct was kindly provided by Dr. Toshiharu Suzuki of Hokkaido University, Japan (Tomita *et al*., 2000). Direct sequencing was carried out to verify the integrity of the inserted DNA sequences. Procedures used to generate, purify and infect replication-deficient *CHFR*-containing recombinant adenoviruses (Ad-CHFR) have been described earlier (Sasaki *et al*., 2001; Satoh *et al*., 2003). A recombinant adenovirus containing the *enhanced green fluorescent proteins* (*EGFP*) gene (Ad-EGFP) was generated as a control.

Antibodies

The anti-Flag monoclonal antibody (M2) was obtained from Sigma (St Louis, MO, USA). The anti-myc monoclonal antibody (9E10); anti-CHFR (sc-13288), anti-p65 (sc-109 and sc-372), anti-p50 (sc-1190), anti-p52 (sc-7386), anti-c-Rel (sc-71) polyclonal antibodies; and horseradish peroxide-conjugated secondary antibodies were obtained from Santa Cruz Biotechnology (Santa Cruz, CA, USA). Anti-p50 (#3035), anti-p52 (#4882) and anti-RelB (#4954) antibodies were obtained from Cell Signaling Technology (Danvers, MA, USA). Alexa 594- and Alexa 488-conjugated secondary antibodies were obtained from Molecular Probes (Carlsbad, CA, USA). The anti-human CXCL8/IL-8 monoclonal antibody (MAB208) was obtained from R&D Systems (Minneapolis, MN, USA). The anti-mouse CD31 monoclonal antibody (MEC13.3) and the biotin-conjugated goat anti-rat, Ig-specific polyclonal antibody were obtained from BD Pharmingen (Franklin Lakes, NJ, USA).

Real-time RT–PCR

Reverse transcription–PCR (RT–PCR) was carried out as described earlier using the TaqMan Gene Expression Assays (Applide Biosystems, Foster City, CA, USA) (Nishikawa *et al*., 2007). Relative levels of gene expression were quantified using the $\Delta\Delta C_t$ method, which calculated the ratio of target gene expression to the expression of glyceraldehyde-3-phosphate dehydrogenase (GAPDH), a housekeeping gene. Primer/probe sets are shown in Supplementary Table S1.

ELISA assays

HCT116 cells were infected with adenovirus Ad-CHFR or Ad-EGFP and cultured in McCoy's 5A medium containing 5% fetal bovine serum. After 32 h, the medium was aspirated and replaced with fresh McCoy's 5A medium containing 5% fetal bovine serum. The cells were then incubated for 16 h, and the conditioned media from Ad-CHFR (CHFR-CM)- or Ad-EGFP (EGFP-CM)-infected cells were collected and centrifuged to remove debris. Conditioned media were analysed in triplicate using a human IL-8-specific ELISA kit (R&D Systems).

Luciferase reporter assays

Cells were plated at a density of 2×10^5 cells per well in 24-well plates. After 24 h, cells were co-transfected with 900 ng of a mammalian expression plasmid or an empty plasmid, in addition to 100 ng of reporter plasmid, pNF-κB-Luc (Stratagene) or human IL-8 promoter–reporter and 2 ng of pRL-TK control reporter vector (Promega, Madison, WI, USA) using LipofectAMINE2000 (Invitrogen, Carlsbad, CA, USA). The pNF-κB-Luc plasmid contains a firefly luciferase reporter gene that was derived from a basic promoter element joined to five tandem repeats of an NF-κB consensus-binding element. Two fragments containing portions of the 5′-regions flanking the IL-8 gene were subcloned upstream of the luciferase reporter gene in the pGL3-Basic vector (Promega). These constructs were named pGL-IL8-54 and pGL-IL8-152 (Figure 4a). Luciferase activities of the reporter plasmids were measured using the Dual-Luciferase Reporter Assay System (Promega), with *Renilla* luciferase activity used as an internal control.

Electrophoretic mobility shift assays

HCT116 cells were infected with Ad-CHFR or Ad-EGFP and cultured in McCoy's 5A medium containing 5% fetal bovine serum for 48 h. Cytoplasmic and nuclear extracts were prepared from the cells using low- and high-salt buffers, respectively, and electrophoretic mobility shift assays (EMSAs) were carried out as described earlier (Kawai *et al*., 2005). The oligonucleotide probe was end-labeled using [γ-^{32}P] ATP (Amersham Biosciences, Piscataway, NJ, USA) and T4 polynucleotide kinase (Roche, Basel, Schweiz).

Colorimetric NF-κB activation assays
Nuclear factor-κB activities were assessed using an ELISA-based colorimetric TransAM NFκB Family kit (Active Motif, Carlsbad, CA, USA). In brief, HCT116 cells were infected with Ad-CHFR or Ad-EGFP and cultured in McCoy's 5A medium containing 5% fetal bovine serum for 48 h. Nuclear extracts were collected using the Nuclear Extract Kit (Active Motif). Equal quantities of total cellular protein (20 μg) were assayed for NF-κB-binding activity using the TransAM NFκB Family Transcription Factor Assay kit (Active Motif), according to the manufacturer's instructions. The wild-type NF-κB and mutated consensus oligonucleotides used in the competition experiments were included at concentrations of 20 pmol per well.

Co-immunoprecipitation assays
Cells were washed with PBS and lysed in HBST buffer (10 mM HEPES (4-(2-hydroxyethyl)-1-piperazineethanesulfonic acid), pH 7.4; 150 mM NaCl, 0.5% Triton X-100, 10 μM MG132, 1 mM NaF, 1 mM Na_3VO_4 and complete protease inhibitor cocktail). The cells were lysed and immunoprecipitated with anti-Flag or with anti-myc antibody.

Immunofluorescence microscopy
Cells (5×10^4) were cultured on four-well chamber slides and transfected using LipofectAMINE2000. After 24 h, the cells were washed with PBS, fixed with 4% paraformaldehyde and incubated with specific primary antibodies at 4 °C overnight. The following day, the cells were incubated with Alexa 594- and Alexa 488-conjugated secondary antibodies at room temperature for 1 h. The labeled cells were examined with an Olympus IX71 fluorescence microscope (Olympus, Tokyo, Japan).

Wound-healing assays
Human umbilical vein endothelial cells were grown to confluence in six-well plates, and the cell monolayer was mechanically scarred using a plastic pipette tip. The cells were washed with fresh EGM-2 medium to remove floating cells and cultured in 1.5 ml of the EGM-2 medium. Conditioned media (100 μl) from CHFR-CM or EGFP-CM were added, with or without 400 ng/ml of anti-IL-8 antibody (MAB208) or 0.1 ng/ml of recombinant human IL-8 (R&D Systems). After 6 or 12 h of incubation at 37 °C and 5% CO_2, cells were visualized under a microscope to assess the movement into the scratched surface.

Migration assays
The migration of HUVECs was assessed by observing the migration of cells through Matrigel-coated transwell inserts, according to the manufacturer's instructions (BD Biosciences, Franklin Lake, NJ, USA). In short, 5×10^4 HUVECs were seeded onto a Matrigel-coated or a control chamber containing growth factor-free EGM-2 medium. Conditioned medium (CHFR-CM or EGFP-CM) was placed in the lower 24-well chamber, with or without 400 ng/ml of anti-IL-8 antibody (MAB208). After 6 h of incubation at 37 °C and 5% CO_2, the chamber interiors were cleaned. The cells on the exterior were fixed and stained using the Diff-Quik kit (Sysmex, Kobe, Japan). The numbers of stained cells that traveled through the Matrigel collagen matrix or through the control membrane were counted under a microscope.

In vivo *tumor formation assay and immunohistochemical examination*
HCT116 cells were subcutaneously injected into 5-week-old BALB/cAJcl-nu/nu mice. For adenoviral injections, Ad-CHFR and Ad-EGFP were purified using the Adeno-X Virus Purification Kit (Clontech, Mountain View, CA, USA), and each virus was intratumoraly injected after tumor cell inoculation. Tumors excised from animals were immunohistochemically stained using an antibody to mouse CD31.

Conflict of interest

The authors declare no conflict of interest.

Acknowledgements

This research was supported by a grant to TT (KAKENHI (20390519)) from the Grants-in-Aid for Scientific Research (B) program of the Japanese Ministry of Education, Culture, Sports, Science and Technology (MEXT). We thank Dr Toshiharu Suzuki (Hokkaido University, Japan) for the pcDNA3-Flag-p65 construct.

References

Akira S, Isshiki H, Sugita T, Tanabe O, Kinoshita S, Nishio Y *et al.* (1990). A nuclear factor for IL-6 expression (NF-IL6) is a member of a C/EBP family. *EMBO J* **9**: 1897–1906.

Boehm JS, Zhao JJ, Yao J, Kim SY, Firestein R, Dunn IF *et al.* (2007). Integrative genomic approaches identify IKBKE as a breast cancer oncogene. *Cell* **129**: 1065–1079.

Cabannes E, Khan G, Aillet F, Jarrett RF, Hay RT. (1999). Mutations in the IkBa gene in Hodgkin's disease suggest a tumour suppressor role for IkappaBalpha. *Oncogene* **18**: 3063–3070.

Campbell SL, Khosravi-Far R, Rossman KL, Clark GJ, Der CJ. (1998). Increasing complexity of Ras signaling. *Oncogene* **17**: 1395–1413.

Cude K, Wang Y, Choi HJ, Hsuan SL, Zhang H, Wang CY *et al.* (2007). Regulation of the G2–M cell cycle progression by the ERK5–NFkappaB signaling pathway. *J Cell Biol* **177**: 253–264.

Cuenca RE, Azizkhan RG, Haskill S. (1992). Characterization of GRO alpha, beta and gamma expression in human colonic tumours: potential significance of cytokine involvement. *Surg Oncol* **1**: 323–329.

Daniels MJ, Marson A, Venkitaraman AR. (2004). PML bodies control the nuclear dynamics and function of the CHFR mitotic checkpoint protein. *Nat Struct Mol Biol* **11**: 1114–1121.

Durocher D, Jackson SP. (2002). The FHA domain. *FEBS Lett* **513**: 58–66.

Emmerich F, Theurich S, Hummel M, Haeffker A, Vry MS, Dohner K *et al.* (2003). Inactivating I kappa B epsilon mutations in Hodgkin/Reed–Sternberg cells. *J Pathol* **201**: 413–420.

Fukuda T, Kondo Y, Nakagama H. (2008). The anti-proliferative effects of the CHFR depend on the forkhead associated domain, but not E3 ligase activity mediated by ring finger domain. *PLoS ONE* **3**: e1776.

Hofmann K, Bucher P. (1995). The FHA domain: a putative nuclear signalling domain found in protein kinases and transcription factors. *Trends Biochem Sci* **20**: 347–349.

Jackson PK, Eldridge AG, Freed E, Furstenthal L, Hsu JY, Kaiser BK *et al.* (2000). The lore of the RINGs: substrate recognition and catalysis by ubiquitin ligases. *Trends Cell Biol* **10**: 429–439.

Kang D, Chen J, Wong J, Fang G. (2002). The checkpoint protein Chfr is a ligase that ubiquitinates Plk1 and inhibits Cdc2 at the G2 to M transition. *J Cell Biol* **156**: 249–259.

Kang D, Wong J, Fang G. (2004). A *Xenopus* cell-free system for analysis of the Chfr ubiquitin ligase involved in control of mitotic entry. *Methods Mol Biol* **280**: 229–243.

Karin M, Cao Y, Greten FR, Li ZW. (2002). NF-kappaB in cancer: from innocent bystander to major culprit. *Nat Rev Cancer* **2**: 301–310.

Kawai N, Takahashi H, Nishida H, Yokosawa H. (2005). Regulation of NF-kappaB/Rel by IkappaB is essential for ascidian notochord formation. *Dev Biol* **277**: 80–91.

Keats JJ, Fonseca R, Chesi M, Schop R, Baker A, Chng WJ *et al.* (2007). Promiscuous mutations activate the noncanonical NF-kappaB pathway in multiple myeloma. *Cancer Cell* **12**: 131–144.

Koch AE, Polverini PJ, Kunkel SL, Harlow LA, DiPietro LA, Elner VM *et al.* (1992). Interleukin-8 as a macrophage-derived mediator of angiogenesis. *Science* **258**: 1798–1801.

Kontermann RE, Munkel S, Neumeyer J, Muller D, Branschadel M, Scheurich P *et al.* (2008). A humanized tumor necrosis factor receptor 1 (TNFR1)-specific antagonistic antibody for selective inhibition of tumor necrosis factor (TNF) action. *J Immunother* **31**: 225–234.

Kunsch C, Rosen CA. (1993). NF-kappa B subunit-specific regulation of the interleukin-8 promoter. *Mol Cell Biol* **13**: 6137–6146.

Lee KH, Bae SH, Lee JL, Hyun MS, Kim SH, Song SK *et al.* (2004). Relationship between urokinase-type plasminogen receptor, interleukin-8 gene expression and clinicopathological features in gastric cancer. *Oncology* **66**: 210–217.

Lenz G, Davis RE, Ngo VN, Lam L, George TC, Wright GW *et al.* (2008). Oncogenic CARD11 mutations in human diffuse large B cell lymphoma. *Science* **319**: 1676–1679.

Libermann TA, Baltimore D. (1990). Activation of interleukin-6 gene expression through the NF-kappa B transcription factor. *Mol Cell Biol* **10**: 2327–2334.

Matsusaka T, Fujikawa K, Nishio Y, Mukaida N, Matsushima K, Kishimoto T *et al.* (1993). Transcription factors NF-IL6 and NF-kappa B synergistically activate transcription of the inflammatory cytokines, interleukin 6 and interleukin 8. *Proc Natl Acad Sci USA* **90**: 10193–10197.

Mumm JB, Oft M. (2008). Cytokine-based transformation of immune surveillance into tumor-promoting inflammation. *Oncogene* **27**: 5913–5919.

Nishikawa N, Toyota M, Suzuki H, Honma T, Fujikane T, Ohmura T *et al.* (2007). Gene amplification and overexpression of PRDM14 in breast cancers. *Cancer Res* **67**: 9649–9657.

Nurnberg W, Tobias D, Otto F, Henz BM, Schadendorf D. (1999). Expression of interleukin-8 detected by in situ hybridization correlates with worse prognosis in primary cutaneous melanoma. *J Pathol* **189**: 546–551.

Ogi K, Toyota M, Mita H, Satoh A, Kashima L, Sasaki Y *et al.* (2005). Small interfering RNA-induced CHFR silencing sensitizes oral squamous cell cancer cells to microtubule inhibitors. *Cancer Biol Ther* **4**: 773–780.

Privette LM, Gonzalez ME, Ding L, Kleer CG, Petty EM. (2007). Altered expression of the early mitotic checkpoint protein, CHFR, in breast cancers: implications for tumor suppression. *Cancer Res* **67**: 6064–6074.

Privette LM, Petty EM. (2008). CHFR: a novel mitotic checkpoint protein and regulator of tumorigenesis. *Transl Oncol* **1**: 57–64.

Rakitina TV, Vasilevskaya IA, O'Dwyer PJ. (2003). Additive interaction of oxaliplatin and 17-allylamino-17-demethoxygeldanamycin in colon cancer cell lines results from inhibition of nuclear factor kappaB signaling. *Cancer Res* **63**: 8600–8605.

Rayet B, Gelinas C. (1999). Aberrant rel/nfkb genes and activity in human cancer. *Oncogene* **18**: 6938–6947.

Rosette C, Karin M. (1995). Cytoskeletal control of gene expression: depolymerization of microtubules activates NF-kappa B. *J Cell Biol* **128**: 1111–1119.

Sasaki Y, Ishida S, Morimoto I, Yamashita T, Kojima T, Kihara C *et al.* (2002). The p53 family member genes are involved in the Notch signal pathway. *J Biol Chem* **277**: 719–724.

Sasaki Y, Morimoto I, Ishida S, Yamashita T, Imai K, Tokino T. (2001). Adenovirus-mediated transfer of the p53 family genes, p73 and p51/p63 induces cell cycle arrest and apoptosis in colorectal cancer cell lines: potential application to gene therapy of colorectal cancer. *Gene Ther* **8**: 1401–1408.

Sathe SS, Sizemore N, Li X, Vithalani K, Commane M, Swiatkowski SM *et al.* (2004). Mutant human cells with constitutive activation of NF-kappaB. *Proc Natl Acad Sci USA* **101**: 192–197.

Satoh A, Toyota M, Itoh F, Sasaki Y, Suzuki H, Ogi K *et al.* (2003). Epigenetic inactivation of CHFR and sensitivity to microtubule inhibitors in gastric cancer. *Cancer Res* **63**: 8606–8613.

Scolnick DM, Halazonetis TD. (2000). Chfr defines a mitotic stress checkpoint that delays entry into metaphase. *Nature* **406**: 430–435.

Smith DR, Polverini PJ, Kunkel SL, Orringer MB, Whyte RI, Burdick MD *et al.* (1994). Inhibition of interleukin 8 attenuates angiogenesis in bronchogenic carcinoma. *J Exp Med* **179**: 1409–1415.

Starczynowski DT, Trautmann H, Pott C, Harder L, Arnold N, Africa JA *et al.* (2007). Mutation of an IKK phosphorylation site within the transactivation domain of REL in two patients with B-cell lymphoma enhances REL's *in vitro* transforming activity. *Oncogene* **26**: 2685–2694.

Tomita S, Fujita T, Kirino Y, Suzuki T. (2000). PDZ domain-dependent suppression of NF-kappaB/p65-induced Abeta42 production by a neuron-specific X11-like protein. *J Biol Chem* **275**: 13056–13060.

Toyota M, Sasaki Y, Satoh A, Ogi K, Kikuchi T, Suzuki H *et al.* (2003). Epigenetic inactivation of CHFR in human tumors. *Proc Natl Acad Sci USA* **100**: 7818–7823.

Wan F, Anderson DE, Barnitz RA, Snow A, Bidere N, Zheng L *et al.* (2007). Ribosomal protein S3: a KH domain subunit in NF-kappaB complexes that mediates selective gene regulation. *Cell* **131**: 927–939.

Williams JL, Ji P, Ouyang N, Liu X, Rigas B. (2008). NO-donating aspirin inhibits the activation of NF-kappaB in human cancer cell lines and Min mice. *Carcinogenesis* **29**: 390–397.

Wu WS, Xu ZX, Hittelman WN, Salomoni P, Pandolfi PP, Chang KS. (2003). Promyelocytic leukemia protein sensitizes tumor necrosis factor alpha-induced apoptosis by inhibiting the NF-kappaB survival pathway. *J Biol Chem* **278**: 12294–12304.

Yasumoto K, Okamoto S, Mukaida N, Murakami S, Mai M, Matsushima K. (1992). Tumor necrosis factor alpha and interferon gamma synergistically induce interleukin 8 production in a human gastric cancer cell line through acting concurrently on AP-1 and NF-kB-like binding sites of the interleukin 8 gene. *J Biol Chem* **267**: 22506–22511.

Yu X, Minter-Dykhouse K, Malureanu L, Zhao WM, Zhang D, Merkle CJ *et al.* (2005). Chfr is required for tumor suppression and Aurora A regulation. *Nat Genet* **37**: 401–406.

Yuan A, Chen JJ, Yao PL, Yang PC. (2005). The role of interleukin-8 in cancer cells and microenvironment interaction. *Front Biosci* **10**: 853–865.

Supplementary Information accompanies the paper on the Oncogene website (http://www.nature.com/onc)

Int. J. Cancer: **124,** 2607–2615 (2009)

Overexpression of Aurora A by loss of CHFR gene expression increases the growth and survival of HTLV-1-infected T cells through enhanced NF-κB activity

Mariko Tomita[1], Minoru Toyota[2], Chie Ishikawa[1,3], Tetsuro Nakazato[1,4], Taeko Okudaira[1,4], Takehiro Matsuda[1,3], Jun-Nosuke Uchihara[5], Naoya Taira[6], Kazuiku Ohshiro[7], Masachika Senba[8], Yuetsu Tanaka[9], Koichi Ohshima[10], Hideyuki Saya[11], Takashi Tokino[2] and Naoki Mori[1]*

[1]*Division of Molecular Virology and Oncology, Graduate School of Medicine, University of the Ryukyus, Nishihara, Okinawa 903-0215, Japan*
[2]*Department of Molecular Biology, Cancer Research Institute, Sapporo Medical University, Sapporo 060-8543, Japan*
[3]*Division of Child Health and Welfare, Faculty of Medicine, University of the Ryukyus, Nishihara, Okinawa 903-0215, Japan*
[4]*Division of Endocrinology and Metabolism, Faculty of Medicine, University of the Ryukyus, Nishihara, Okinawa 903-0215, Japan*
[5]*Department of Internal Medicine, Naha City Hospital, Naha, Okinawa 902-8511, Japan*
[6]*Department of Internal Medicine, Heart Life Hospital, Nakagusuku, Okinawa 901-2492, Japan*
[7]*Department of Internal Medicine, Okinawa Prefectural Nanbu Medical Center and Children's Medical Center, Haebaru, Okinawa 901-1193, Japan*
[8]*Department of Pathology, Institute of Tropical Medicine, Nagasaki University, Nagasaki 852-8523, Japan*
[9]*Division of Immunology, Faculty of Medicine, University of the Ryukyus, Nishihara, Okinawa 903-0215, Japan*
[10]*Department of Pathology, School of Medicine, Kurume University, Kurume 830-0011, Japan*
[11]*Division of Gene Regulation, Institute for Advanced Medical Research, Keio University School of Medicine, Tokyo 160-8582, Japan*

Human T-cell leukemia virus type 1 (HTLV-1) is the etiologic agent for adult T-cell leukemia (ATL). Aurora A, a mitotic checkpoint protein, is overexpressed in human cancer cells. The cell cycle-dependent turnover of Aurora A is regulated by E3 ubiquitin ligases such as checkpoint with fork head-associated and ring finger (CHFR). Here, we found overexpression of Aurora A protein in HTLV-1-infected T-cell lines and primary ATL cells. The expression of CHFR mRNA was reduced in these cells by abnormal methylation of *CHFR* promoter region. Knockdown of Aurora A using small interfering RNA suppressed the growth of HTLV-1-infected T-cell line. Transfection of Aurora A expression plasmid enhanced Tax-induced nuclear factor-κB (NF-κB) reporter activity. Transfection of CHFR expression plasmid into an HTLV-1-infected T-cell line reduced cell growth, Aurora A protein level and constitutive NF-κB reporter activity. Aurora kinase inhibitor suppressed the growth and survival of HTLV-1-infected T-cell lines and primary ATL cells. It also reduced constitutive NF-κB activity in an HTLV-1-infected T-cell line by reducing IκB kinase β phosphorylation and the expression of antiapoptotic protein survivin. Our results suggested that loss of CHFR expression resulted to accumulation of Aurora A, which increased NF-κB activity. These findings highlight the critical role of Aurora A in HTLV-1-infected T cells, making this molecule a potentially suitable target for future therapies for ATL.

Key words: Aurora A; Aurora kinase inhibitor; HTLV-1; ATL; CHFR

The *Aurora A* gene encodes a centrosome-associated serine/threonine kinase.[1] There are 3 mammalian Aurora kinase genes, encoding Aurora A, B and C. The Aurora kinases play a regulatory role from G_2 through to cytokinesis.[2] Aurora A is mainly localized at spindle poles and the mitotic spindle during mitosis, where it regulates the functions of centrosomes, spindles and kinetochores required for proper mitotic progression. Preclinical studies have demonstrated the oncogenic potential of Aurora A activation resulting in transformation of rodent fibroblast cells and the formation of multipolar mitotic spindles inducing genomic instability.[3] Indeed, the Aurora A gene is amplified and overexpressed in human cancers originating from multiple tissue types.[4] Overexpression of Aurora A has been shown to induce resistance to tubulin-targeted antitumor agents, such as paclitaxel, by enhancing the mitotic spindle formation during mitosis.[5] The link between Aurora A overexpression and aneuploidy has led to the concept that overexpression of Aurora A may be responsible for the acquisition of other genetic alterations required for carcinogenesis.[6] However, the exact role of Aurora A in carcinogenesis remains elusive since little is known about its biochemical targets. Some of the known substrates or interacting proteins of Aurora A, such as c-Myc, telomerase, p53 and BRCA1, could be important mediators in carcinogenesis.[7] These properties make the Aurora kinases attractive targets for anticancer therapy; indeed, the first inhibitors have entered the clinical trial phase.[8]

Aurora A expression is regulated by cell-cycle dependent manner. Several proteins, which have ubiquitine ligase activity such as checkpoint with fork head-associated and ring finger (CHFR), have been reported to regulate Aurora A protein stability.[9] CHFR is an early mitotic checkpoint protein that initiates cell cycle delay in response to microtubule stress during prophase in mitosis.[10] Previously, Yu *et al.*[9] showed that mice lacking the *CHFR* gene develops leukemia and are prone to chemically-induced skin cancer, suggesting that *CHFR* is a tumor suppressor gene.[9] CHFR protein interacts with and ubiquitinates Aurora A, resulting in reduction of Aurora A protein.[9] CHFR deficiency results in chromosomal instability in embryonic fibroblasts through upregulation of Aurora A, implying that disruption of the CHFR-Aurora A interaction causes chromosomal instability.[9] Taken together,

Abbreviations: ATL, adult T-cell leukemia; CHFR, checkpoint with fork head-associated and ring finger; COBRA, combined bisulfite restriction analysis; EMSA, electrophoretic mobility shift assay; HTLV-1, human T-cell leukemia virus type 1; IKK, IκB kinase; IL-2R, interleukin-2 receptor; NF-κB, nuclear factor-κB; PBMCs, peripheral blood mononuclear cells; RT-PCR, Reverse transcriptase PCR; siRNA, small interfering RNA.

Grant sponsor: Ministry of Education, Culture, Sports, Science and Technology of Japan; Grant number: 19591122; Grant sponsors: Foundation for Promotion of Cancer Research in Japan, Uehara Memorial Foundation, Public Trust Haraguchi Memorial Cancer Research Fund, Takeda Science Foundation, Japan Leukemia Research Fund; Grant sponsor: Princes Takamatsu Cancer Research Fund; Grant number: 07-23905.

***Correspondence to:** Division of Molecular Virology and Oncology, Graduate School of Medicine, University of the Ryukyus, Nishihara, Okinawa 903-0215, Japan. E-mail: n-mori@med.u-ryukyu.ac.jp

Received 26 August 2008; Accepted after revision 23 December 2008
DOI 10.1002/ijc.24257
Published online 12 January 2009 in Wiley InterScience (www.interscience.wiley.com).

Aurora A and CHFR have antagonistic roles in the control of cell viability. A balance of quantity and activity between Aurora A and CHFR might be important in maintaining a normal growth rate of cells. There is ample evidence to suggest that CHFR acts as a tumor suppressor, and that loss of CHFR expression, occasionally due to hypermethylation of *CHFR* promoter region, is evident in cancer cells but not in normal tissues.[11]

Adult T-cell leukemia (ATL) is an aggressive malignant disease of CD4-positive T lymphocytes caused by infection with human T-cell leukemia virus type I (HTLV-1).[12–14] HTLV-1 causes ATL in 3–5% of infected individuals after a long-latent period of 40–60 years.[15] ATL remains of poor prognosis with a median survival time of 13 months in aggressive ATL.[16] Conventional therapies do not seem to prolong survival of patients with ATL,[17] and the development of new therapeutic strategies for ATL is necessary. Because of the low incidence and long latency of ATL, leukemogenesis is thought to be a multistep process. In HTLV-1-expressing cells, the virus-encoded transforming protein, Tax, plays a critical role in the growth and survival of infected T cells by perturbing normal regulatory mechanisms, resulting in uncontrolled cell growth.[18] Tax activates many cellular transcription factors including nuclear factor-κB (NF-κB).[18] NF-κB is a key transcription factor involved in the expression of genes that play key roles in growth, apoptosis and tumorigenesis of many human cancer cells including HTLV-1-infected T cells.[19,20] The classical pathway of NF-κB activation involves the IκB kinase (IKK) complex [IKKα, IKKβ and IKKγ (NEMO)] responsible for phosphorylation of IκB.[21] Normally, IκB sequesters NF-κB in the cytoplasm, but when phosphorylated, IκB is targeted for proteolysis, resulting in the nuclear translocation and activation of NF-κB complexes.[21] Tax activates NF-κB pathways by physically targeting IKK complexes.[19]

In addition to dysregulation of cellular NF-κB signaling pathways, HTLV-1-infected T-cell lines and ATL cells show dysregulation of mitotic checkpoint proteins,[22,23] and HTLV-1 Tax is known to affect centrosome numbers.[24] Aurora A is involved in centrosome duplication, and abnormal centrosomal duplication is important for retroviral pathogenesis.[25] Recent studies have suggested that Aurora A activates NF-κB signaling pathway in some cancer cell lines.[26,27] In this study, we investigated the effects of Aurora A on the growth and survival of HTLV-1-infected T-cell lines and primary ATL cells, with a special focus on NF-κB signaling pathway.

Material and methods

Reagents

Pan-Aurora kinase inhibitor, 4-(4′-Benzamidoanilino)-6, 7-dimethoxyquinazoline and DNA methyltransferase inhibitor, 5-aza-2-Deoxycytidine, was purchased from Calbiochem (La Jolla, CA). DNA synthesis inhibitor, hydroxyurea, was obtained from Sigma-Aldrich (St. Louis, MO).

Antibodies

We used primary antibodies against Tax (Lt-4),[28] anti-Aurora A and Aurora B antibodies (BD Biosciences, San Jose, CA), anti-phospho-IKKβ (Ser181), IKKβ, phospho-IκBα (Ser32/36), PARP (Cleaved PARP Asp214) and survivin antibodies (Cell Signaling Technology, Beverly, MA), anti-IκBα antibody (Santa Cruz Biotechnology, Santa Cruz, CA), anti-Cyclin B1 and actin antibodies (Lab Vision, Fremont, CA) and anti-Flag antibody (Sigma-Aldrich). Horseradish-peroxidase-conjugated secondary antibodies were purchased from GE Healthcare (Waukesha, WI).

Cell lines

The HTLV-1-uninfected T-cell leukemia cell lines Jurkat and MOLT-4, the HTLV-1-infected T-cell lines MT-2,[29] MT-4,[30] SLB-1[31] and HUT-102[12] were maintained in RPMI 1640 medium supplemented with 10% heat-inactivated fetal bovine serum, 50 IU/mL penicillin and 50 μg/mL streptomycin (Sigma-Aldrich) at 37°C in 5% CO_2. MT-2, MT-4 and SLB-1 are HTLV-1-transformed T-cell lines, established by an *in vitro* coculture protocol. HUT-102 was established from a patient with ATL, but it was not clear whether HUT-102 cells represent the tumor clone from the donor ATL patient.

Clinical samples

The diagnosis of ATL was based on clinical features, hematological findings and the presence of anti-HTLV-1 antibodies in the sera. Monoclonal HTLV-1 provirus integration into the DNA of leukemia cells was confirmed by Southern blot hybridization in all patients (data not shown). Each ATL sample contained 78–89% of leukemia cells morphologically at the time of analysis. Peripheral blood mononuclear cells (PBMCs) from healthy volunteers (n = 2) and patients with ATL (n = 17) were isolated by Ficoll-Paque density gradient centrifugation (GE Healthcare). Lymph nodes samples (n = 10) were also obtained from 10 patients with ATL for analysis of Aurora A protein expression. The study protocol was approved by the Human Ethics Review Committee of University of the Ryukyus, and all samples were obtained after informed consent.

Western blot analysis

Western blot analysis was performed as described previously.[32] In brief, whole cell lysates were subjected to SDS-PAGE and electroblotted onto polyvinylidene difluoride membranes (Millipore, Billerica, MA), and then analyzed for immunoreactivity with the appropriate primary and secondary antibodies as indicated in the figures. Reaction products were visualized using Enhanced Chemiluminescence reagent, according to the instructions provided by the manufacturer (Amersham Pharmacia, Uppsala, Sweden).

Reverse transcriptase PCR

Total cellular RNA was extracted from cells using Trizol (Invitrogen, Carlsbad, CA) as described by the supplier. First-strand cDNA was synthesized in a 10-μL reaction volume using RNA-PCR kit (TAKARA BIO, Ohtsu, Japan) with random primers. Thereafter, cDNA was amplified for Aurora A, CHFR and β-actin. The oligonucleotide primers used were as follows: for Aurora A, sense, 5′-GTCTTGTGTCCTTCAAATTCTTC-3′ and antisense, 5′-TCTTTTGGGTGTTATTCAGTGGC-3′, for CHFR; sense, 5′-GCATGTCAGCGTCTCCTCCATCTTG-3′ and antisense, 5′-GGCGAGAGCGTTCCTCCAGTTG-3′; and for β-actin; sense, 5′-GTGGGGCGCCCCAGGCACCA-3′ and antisense, 5′-CTCCTTA-ATGTCACGCACGATTTC-3′. Product sizes were 154-bp for Aurora A, 317-bp for CHFR and 548-bp for β-actin. The amplification programs were as follow: for Aurora A; denaturing at 94°C for 1 min, an annealing step at 56°C for 1 min and an extension step at 72°C for 1 min, for 27 cycles, for CHFR; denaturing at 94°C for 1 min, an annealing step at 60°C for 1 min and an extension step at 72°C for 1 min, for 30 cycles, for β-actin; denaturing at 94°C for 30 sec, an annealing step at 60°C for 30 sec and an extension step at 72°C for 90 sec for 28 cycles. The PCR products were fractionated on 2% agarose gels and visualized by ethidium bromide staining.

Immunohistochemical analysis

Serial sections of lymph nodes samples were deparaffinized in xylene and dehydrated using a graded ethanol series. For better detection, sections of lymph nodes samples were pretreated with ready-to-use proteinase K (Dako, Carpinteria, CA) for 20 min at 37°C. This procedure increased the number of antigenic sites available for binding by the antibody. In the next step, the lymph nodes sections were placed in 3% hydrogen peroxide and absolute methanol for 5 min to reduce endogenous peroxidase activity, followed by washing in PBS. The lymph nodes sections were incubated with antihuman Aurora A polyclonal antibody (diluted 1:250) or a control mouse immunoglobulin G for 3 hr at 37°C.

After washing with PBS, the sections were covered with EnVision plus (Dako) for 40 min at 37°C and washed in PBS. Antigenic sites bound by the antibody were identified by reacting the sections with a mixture of 0.05% 3,3′-diaminobenzidine tetrahydrochloride in 50 mM Tris-HCl buffer and 0.01% hydrogen peroxide for 7 min. Sections were then counterstained with methyl green for 10 min, hydrated in ethanol, cleaned in xylene and mounted.

Transfection

Transfection was performed by using MicroPorator MP-100™ (Digital Bio Technology, Seoul, Korea) according to the instructions supplied by the manufacturer for optimization and use.

Small interfering RNA

To knockdown Aurora A expression, a pre-designed double-stranded small interfering RNA (siRNA; Santa Cruz Biotechnology) was used. A siCONTROL nontargeting siRNA pool (Dharmacon, Lafayette, CO) was used as a negative control. siRNAs were transfected into Jurkat or HUT-102 cells at a final concentration of 100 nM. Transfected cells were incubated for 12 hr, seeded into 24-well plates at 0.5 or 1×10^5 viable cells per well, and incubated for the indicated times. The number of viable cells was determined every 24 hr by counting Trypan Blue excluding cells in a hemocytometer.

Plasmids

The expression plasmid for HTLV-1 Tax was kindly provided by Dr K Matsumoto.[33] The expression plasmids for wild type and kinase dead mutant (K162M, in which Lys162 in the ATP binding site is replaced with Met) of Aurora A were described previously.[34] Flag tagged CHFR expression plasmid was described previously.[11] Reporter plasmid κB-LUC is a luciferase expression plasmid controlled by five tandem repeats of the NF-κB binding sequences of the *interleukin-2 (IL-2) receptor (IL-2R) α-chain* gene.

Luciferase assay

Cells were transiently transfected with the indicated effecter plasmids and a luciferase reporter construct. In all cases, the reference plasmid phRL-TK (Promega, Madison, WI), which contains the *Renilla* luciferase gene under the control of the tymidine kinase promoter, was cotransfected to correct for transfection efficiency. Luciferase assays were performed by using the Dual-Luciferase Reporter System (Promega), in which relative luciferase activities were calculated by normalizing transfection efficiency according to the Renilla luciferase activities.

Cellular proliferation assay

Proliferation of T-cell lines after treatment with the Aurora kinase inhibitor, and transfection of Aurora A siRNA or CHFR expression plasmid was analyzed by counting viable cells using Trypan Blue exclusion method. The antiproliferative effects of Aurora kinase inhibitor against primary ATL cells and PBMCs of healthy donors were measured by the WST-8 method (Cell Counting Kit-8; Wako Pure Chemical Industries, Osaka, Japan) based on the MTT assay, as described previously.[35] Briefly, the 5×10^3 cells were incubated in triplicate in a 96-well microculture plate in the presence of different concentrations of Aurora kinase inhibitor (0, 2.5 or 10 μM) in a final volume of 0.1 mL for 48 hr at 37°C. Thereafter, 5 μL Cell Counting Kit-8 solution (5 mM WST-8, 0.2 mM 1-methoxy 5-methylphenazinium methylsulfate and 150 mM NaCl) was added, and the cells were further incubated for another 4 hr. The number of surviving cells was measured by a 96-well multiscanner autoreader at optical density of 450 nm. Cell viability was determined as percentage of the control (absence of Aurora kinase inhibitor).

Cell cycle analysis

Cell cycle analysis was performed with the CycleTEST PLUS DNA reagent kit (Becton Dickinson, San Jose, CA). In brief, cells were washed with a buffer solution containing sodium citrate, sucrose and dimethyl sulfoxide, suspended in a solution containing RNase A, and stained with 125 μg/mL propidium iodide for 10 min. Cell suspensions were analyzed on a Epics XL-MCL flow cytometer (Beckman Coulter, Fullerton, CA) using EXPO32 software. The cell population at each cell cycle phase was determined with MultiCycle software.

Apoptosis assay

Cells were plated at a density of 1×10^5 cells/mL in 60-mm tissue culture dish. Twelve hours after plating, cells were exposed to Aurora kinase inhibitor (10 μM) for 24 hr. Apoptosis was quantified by staining with Annexin-V-Fluos (Roche Diagnostics, Mannheim, Germany) according to instructions provided by the manufacturer followed by analysis on a Epics XL-MCL flow cytometer using EXPO32 software.

Electrophoretic mobility shift assay

Nuclear extracts were prepared from Aurora kinase inhibitor-treated and untreated cells. NF-κB, AP-1 and Oct-1 binding activity was analyzed by electrophoretic mobility shift assay (EMSA) as described previously.[36] The probes used were prepared by annealing the following sense and antisense synthetic oligonucleotides: a typical NF-κB element from the *IL-2R α chain* gene (5′-gatcCGGCAG*GGGAATCTCC*CTCTC-3′), an AP-1 element of the *IL-8* gene (5′-gatcGTGA*TGACTCA*GGTT-3′). The oligonucleotide 5′-gatcTGTCGA*ATGCAAAT*CACTAGAA-3′, containing the consensus sequence of the octamer binding motif, was used to identify specific binding of the transcription factor Oct-1. Italic sequences represent the NF-κB, AP-1 or Oct-1 binding sites.

Bisulfite treatment and combined bisulfite restriction analysis

Genomic DNA was purified from cells by using Blood & Tissue Genomic DNA Extraction Miniprep System (Viogene, Taipei, Taiwan) as described by the supplier. Genomic DNA was initially treated with sodium bisulfite (Sigma-Aldrich) and combined bisulfite restriction analysis (COBRA), a semiquantitative methylation assay, was carried out as described previously.[37,38] Briefly, bisulfite PCR was carried out with primers that amplify both methylated and unmethylated alleles. After bisulfite treatment, the PCR products were digested with restriction enzyme, NrUI, that cleave exclusively methylated CpG sites (Fig. 2*c* right panel). The PCR primers used were as follows: sense, 5′-YGTTTATTAAGAG-YGGTAGTTAAAG-3′ (Y; C or T) and antisense, 5′-AAAATCC-TTAAAACTTCCAATCC-3′. The amplification program was; denaturing at 94°C for 1 min, an annealing step at 53°C for 1 min, for 3 cycles, at 51°C for 1 min, for 4 cycles, at 49°C for 1 min, for 5 cycles, at 47°C for 1 min, for 26 cycles and an extension step at 72°C for 1 min in each annealing steps.

Statistical analysis

Data were expressed as mean ± SD. For data analysis, the unpaired Student's *t*-test was used. A p value less than 0.05 denoted the presence of a statistically significant difference.

Results

Overexpression of Aurora A protein in HTLV-1-infected T-cell lines and primary ATL cells

We first analyzed the expression of Aurora A in HTLV-1-infected and uninfected T-cell lines. The expression level of Aurora A protein was higher in each HTLV-1-infected T-cell line compared with uninfected T-cell lines (Fig. 1*a*). We also observed high Aurora A expression in 2 out of 6 PBMC samples from primary ATL patients (Fig. 1*a*). Furthermore, lymph nodes samples from patients with ATL also stained positive for Aurora A,

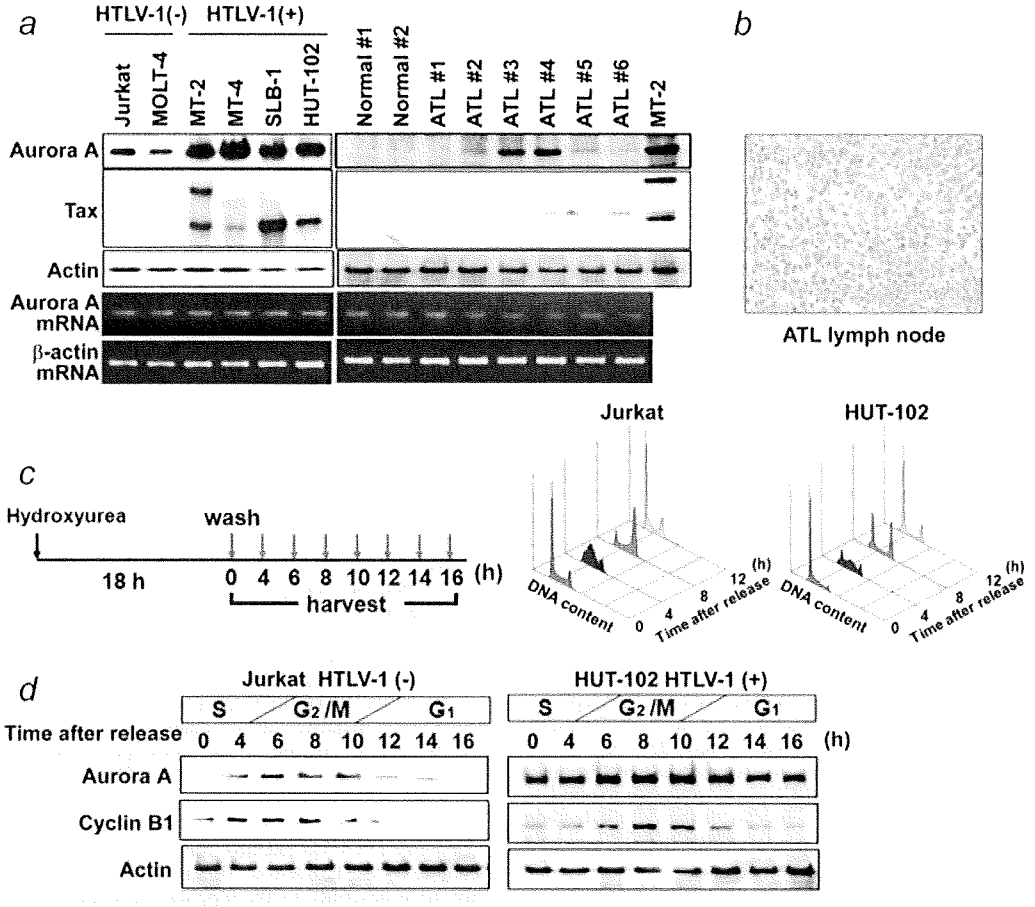

FIGURE 1 – Overexpression of Aurora A in HTLV-1-infected T-cell lines and primary ATL cells. (*a*) Aurora A and Tax protein expressions in HTLV-1-infected T-cell lines [HTLV-1(+)], uninfected T-cell lines [HTLV-1(−)], PBMCs from patients with ATL (ATL 1–6) and those from healthy donors (Normal 1 and 2) were analyzed by western blotting. Actin expression served as a control. Aurora A mRNA expression was analyzed by RT-PCR (second panels from the bottom). β-actin was a loading control (bottom panels). (*b*) Immunohistochemical staining of Aurora A in a lymph node from a patient with ATL. Original magnification, ×200. (*c*) Jurkat and HUT-102 cells were synchronized with hydroxyurea (1 mM, for 18 hr) at early S phase, and collected at the indicated times after release from arrest (left panel). Cell cycle synchronization after release from cell cycle arrest was confirmed by flow cytometry (right panels). (*d*) Expression of Aurora A in Jurkat and HUT-102 cells after release from cell cycle arrest was determined by western blot. Cyclin B1 is a marker of G_2/M phase. Antibody against actin was used as an equal-loading control. Representative results of three experiments with similar findings.

although normal lymph node samples stained almost negative (Fig. 1*b* and data not shown). The specificity of the monoclonal antibody was confirmed when control tissues were stained with mouse IgG, and none showed any staining (data not shown). On the other hand, the mRNA level of Aurora A determined by reverse transcriptase PCR (RT-PCR) was comparable in HTLV-1-infected and uninfected T-cell lines. It was also comparable in PBMCs from patients with ATL and those from healthy donors (Fig. 1*a*). There was no correlation between Aurora A and Tax protein expression levels (Fig. 1*a*).

Loss of cell cycle-dependent regulation of Aurora A expression in HTLV-1-infected T cells

Under normal conditions, expression of Aurora A protein is tightly regulated in a cell cycle-dependent manner.[39] We next analyzed whether the expression of Aurora A protein in HTLV-1-infected T-cell lines is regulated in a cell cycle-dependent manner or not. The cell cycles of Jurkat and HUT-102 cells were synchronized by treatment with hydroxyurea then released from early S phase. The protocol for hydroxyurea treatment is summarized in the left panel of Fig. 1*c*. Cell cycle synchronization was confirmed by flow cytometry (Fig. 1*c*, right panels). Consistent with the earlier findings,[39] Aurora A protein in Jurkat cells was almost absent through G_1, began to accumulate in late S phase and reached a peak level in mitosis in a manner similar to that of cyclin B1, a marker of mitosis (Fig. 1*d*, left panels). In contrast, the level of Aurora A protein in HUT-102 cells was stable during the G_1/S phase (Fig. 1*d*, right panels). These results suggest that in HTLV-1-infected T cells, Aurora A protein expression is not regulated by cell cycle-related mechanisms, implying that this protein might play an additional role in HTLV-1-induced leukemogenesis.

Loss of CHFR expression by aberrant methylation is associated with accumulation of Aurora A

To elucidate the mechanism of Aurora A protein accumulation in HTLV-1-infected T cells, we focused on CHFR. We found negative expression of CHFR mRNA in all HTLV-1-infected T-cell lines, although the expression was detectable in uninfected T-cell lines (Fig. 2*a*). The expression was also suppressed in PBMCs from patients with ATL compared with those from healthy donors (Fig. 2*a*). However the levels of decrease of CHFR in ATL cells